

Accession of Tumor Heterogeneity by Multiplex Transcriptome Profiling of Single Circulating Tumor Cells

Tobias M. Gorges,^{1††} Andra Kuske,^{1†} Katharina Röck,¹ Oliver Mauermann,¹ Volkmar Müller,² Sven Peine,³ Karl Verpoort,⁴ Vendula Novosadova,⁵ Mikael Kubista,^{5,6} Sabine Riethdorf,¹ and Klaus Pantel^{1*}

BACKGROUND: Transcriptome analysis of circulating tumor cells (CTCs) holds great promise to unravel the biology of cancer cell dissemination and identify expressed genes and signaling pathways relevant to therapeutic interventions.

METHODS: CTCs were enriched based on their EpCAM expression (CellSearch[®]) or by size and deformability (ParsortixTM), identified by EpCAM and/or pan-keratin-specific antibodies, and isolated for single cell multiplex RNA profiling.

RESULTS: Distinct breast and prostate CTC expression signatures could be discriminated from RNA profiles of leukocytes. Some CTCs positive for epithelial transcripts (*EpCAM* and *KRT19*) also coexpressed leukocyte/mesenchymal associated markers (*PTPRC* and *VIM*). Additional subsets of CTCs within individual patients were characterized by divergent expression of genes involved in epithelial-mesenchymal transition (e.g., *CDH2*, *MMPs*, *VIM*, or *ZEB1* and 2), DNA repair (*RAD51*), resistance to cancer therapy (e.g., *AR*, *AR-V7*, *ERBB2*, *EGFR*), cancer stemness (e.g., *CD24* and *CD44*), activated signaling pathways involved in tumor progression (e.g., *PIK3CA* and *MTOR*) or cross talks between tumors and immune cells (e.g., *CCL4*, *CXCL2*, *CXCL9*, *IL15*, *IL1B*, or *IL8*).

CONCLUSIONS: Multimarker RNA profiling of single CTCs reveals distinct CTC subsets and provides important insights into gene regulatory networks relevant for cancer progression and therapy.

© 2016 American Association for Clinical Chemistry

Detection and molecular characterization of circulating tumor cells (CTCs)⁷ could provide valuable information for the clinical management of cancer patients because CTCs represent a real-time snapshot of the current tumor burden (1). Mutational analysis of CTCs might help to investigate alterations in genes involved in the response to targeted therapies (2, 3), which supports the use of CTCs as a “liquid biopsy.”

However, to identify signaling pathways and splice variants relevant to cancer biology and therapies, transcriptome analysis of viable cancer cells is essential (4). Quantitative real-time PCR (qPCR) targeting keratin19 (*KRT19*)⁸ has been widely used to detect and monitor CTCs in cancer patients (5, 6). However, single marker analysis is not sufficient to understand the broad and complex nature of tumor biology. So far, multiplex qPCR targeting a few transcripts of interest has been applied (7, 8). However, most reports have relied on CTC-enriched fractions that still contain substantial numbers of contaminating leukocytes. Moreover, analy-

¹ Department of Tumor Biology, University Medical Center Hamburg-Eppendorf, Hamburg, Germany; ² Department of Gynecology, University Hospital Hamburg-Eppendorf, Hamburg, Germany; ³ Department of Transfusion Medicine, University Hospital Hamburg-Eppendorf, Hamburg, Germany; ⁴ Practice for Haematology and Oncology, Hamburg, Germany; ⁵ Department of Biotechnology, Czech Academy of Sciences, Prague, Czech Republic; ⁶ TATAA Biocenter, Gothenburg, Sweden.

* Address correspondence to: T.M.G. and K.P. at Department of Tumor Biology, University Medical Center Hamburg-Eppendorf, Hamburg, Germany. Fax: +49-(0)40-7410-55379; e-mail t.gorges@uke.de or pantel@uke.de.

† T.M. Gorges and A. Kuske contributed equally to this work.

Received May 18, 2016; accepted August 15, 2016.

Previously published online at DOI: 10.1373/clinchem.2016.260299

© 2016 American Association for Clinical Chemistry

⁷ Nonstandard abbreviations: CTCs, circulating tumor cells; qPCR, quantitative real-time PCR; EMT, epithelial-mesenchymal transition; Cq, quantification cycle; PCA, principal component analysis.

⁸ Human genes: *KRT19*, keratin19; *EPCAM*, epithelial cell adhesion molecule; *EGFR*, epidermal growth factor receptor; *ERBB2*, erb-b2 receptor tyrosine kinase 2; *ACTB*, β -Actin;

CDH1_1, cadherin 1_1; *SCGB2A1*, secretoglobulin family 2A member 1; *ESR1*, estrogen receptor 1; *EMP2*, epithelial membrane protein 2; *PTPRC*, protein tyrosine phosphatase, receptor type C; *VIM*, vimentin; *PIK3CA*, phosphatidylinositol-4,5-bisphosphate 3-kinase catalytic subunit alpha; *MTOR*, mechanistic target of rapamycin; *CD44*, CD44 molecule (Indian blood group); *WHSC1*, Wolf-Hirschhorn syndrome candidate 1; *CDH2*, cadherin 2; *COL1A2*, collagen type I alpha 2 chain; *COL5A2*, collagen type V alpha 2 chain; *FN1*, fibronectin 1; *MAP1B*, microtubule associated protein 1B; *MMP3*, matrix metalloproteinase 3; *SOX10*, SRY-box 10; *SPP1*, secreted phosphoprotein 1; *ZEB1*, zinc finger E-box binding homeobox 1; *ZEB2*, zinc finger E-box binding homeobox 2; *VEGFA*, vascular endothelial growth factor A; *NF- κ B*, nuclear factor κ B; *NKX3-1*, NK3 homeobox 1; *TMPPRSS2-ERG*, ERG, ETS transcription factor; *TMPPRSS2*, transmembrane protease, serine 2; *RAD51*, RAD51 recombinase; *AR-V7*, androgen receptor V7; *STAT3*, signal transducer and activator of transcription 3; *CCL4*, C-C motif chemokine ligand 4; *CXCL2*, C-X-C motif chemokine ligand 2; *IL15*, interleukin 15; *Twist*, twist family bHLH transcription factor; *ABCC1*, ATP binding cassette subfamily C member 1; *ADAM17*, ADAM metalloproteinase domain 17.

ses of pooled CTC fractions miss the information on inpatient heterogeneity of CTC populations.

Isolation of single CTCs and subsequent RNA analysis is challenging but the information obtained is much more extensive with regard to tumor cell heterogeneity in individual patients. A dual colorimetric RNA in situ hybridization assay was recently used to examine individual CTCs and tumor cell clusters for the expression of epithelial transcripts and mesenchymal markers (9). Heterogeneous RNA expression of single CTCs has also been demonstrated in patients with prostate cancer using the CTC-iChip for CTC isolation that is not commercially available (10).

In this study we performed single cell analysis after EpCAM-dependent (CellSearch[®], Janssen Diagnostics) or size-based (Parsortix[™], ANGLE Plc) enrichment. We established a workflow to screen up to 84 genes specific for different tumor entities, genes involved in DNA repair, epithelial–mesenchymal transition (EMT), tumor suppressor genes, therapy-related targets, stem cell-related markers, transcripts of activated signaling pathways, or genes mediating cross talk between tumors and immune cells.

Materials and Methods

CELL CULTURE

All cells [MDA-MB-468 (MDA-468), MDA-MB-231 (MDA-231), SKBR-3 and MCF7] were obtained from the American Type Culture Collection proposed by the vendor. Cells were harvested when they reached a confluence of approximately 80%.

RNA ISOLATION, cDNA SYNTHESIS, AND qPCR

Total RNA (500 ng) from MDA-468, MDA-231, SKBR3, and MCF7 cells was isolated using the RNeasy Micro Kit (QIAGEN) according to the protocol of the vendor. To generate first-strand cDNA, 0.5 μ g of total RNA was reverse transcribed using the First-Strand cDNA Synthesis Kit (Thermo Scientific). Qualitative PCR was performed in a peqStar Thermocycler (Peqlab) under the following conditions: after 10 min denaturation at 95 °C, 35 cycles were carried out by denaturation at 94 °C for 30 s, annealing at 60 °C for 30 s, and elongation for 30 s at 72 °C. After a final elongation step at 72 °C for 10 min the samples were stored at 4 °C. Ethidium bromide stained-agarose gel electrophoresis was used to confirm the formation of the expected PCR products. (See Fig. 1 in the Data Supplement that accompanies the online version of this article at <http://www.clinchem.org/content/vol62/issue12>.)

Primers were designed using the Primer3 software [epithelial cell adhesion molecule (*EpCAM*): forward 5'-GCTGGTGTGTGAACACTGCT-3' and reverse 5'-ACGCGTTGTGATCTCCTTCT-3'; epidermal

growth factor receptor (*EGFR*): forward 5'-CAGCGCTACCTTGTCATTCA-3' and reverse 5'-TGCACTCAGAGAGCTCAGGA-3'; erb-b2 receptor tyrosine kinase 2 (*ERBB2*): forward 5'-TGCCTGTCCCTACAACCTACC-3' and reverse 5'-CAGACCATAGACCACTCGG; *KRT19*: forward 5'-CAGCGCTACCTTGTCATTCA-3' and reverse 5'-GATCTGCATCTCCAGGTCGG-3'; and β -Actin (*ACTB*): forward 5'-CCAACCGCGAGAAGATGA-3' and reverse 5'-CCAGAGGCGTACAGGGATAG-3'].

ENRICHMENT OF TUMOR CELLS FOR SINGLE CELL RNA ANALYSIS

CellSearch Epithelial Cell Profile Kit. The CellSearch Epithelial Cell Profile Kit (Janssen Diagnostics) contains a ferrofluid-based capture reagent coated to antibodies targeting the EpCAM antigen. EDTA blood samples were processed without fixation or permeabilization.

Parsortix System. The Parsortix (ANGLE Plc) is a marker-independent system for tumor cell enrichment capturing intact and viable tumor cells based on their size ($\geq 10 \mu$ m) (11).

STAINING AND ISOLATION OF THE TUMOR CELLS

To distinguish tumor cells from the leukocytes, an epithelial-cell specific staining protocol was established targeting EpCAM and/or pan-keratins (EpCAM and pan-keratins for CTCs isolated by Parsortix and pan-keratins for tumor cells isolated by CellSearch). Briefly, enriched tumor cells were eluted into Eppendorf tubes, stained, and isolated by micromanipulation for single cell analysis.

The EpCAM antibody (Novocastra) was diluted in 10% AB-Serum/PBS (1:100) and incubated for 45 min on a rotor. Next, the sample was washed and a fluorescently labeled secondary antibody (Thermo Fisher) was added (1:150) for another 30 min in the dark. For subsequent pan-keratin staining, samples were washed and the CellSearch monoclonal pan-keratin antibody cocktail (included in the CellSearch Circulating Epithelial Cell Kit) was added (1:10; incubation time 20 min in the dark). Stained cells were washed and transferred onto a glass slide for single cell isolation by micromanipulation (2).

TESTING OF DIFFERENT KITS FOR SINGLE CELL ANALYSIS

We tested the NucleoSpin RNA II Kit[®] (Macherey-Nagel), the Picopure RNA Isolation Kit[®] (Life Technologies), the MessageBooster Kit[™] (Epicentre), and the CelluLyser[™] Micro Lysis and cDNA Synthesis Kit (TATAA Biocenter) for single cell analysis. Kits were applied according to the instructions of the vendors.

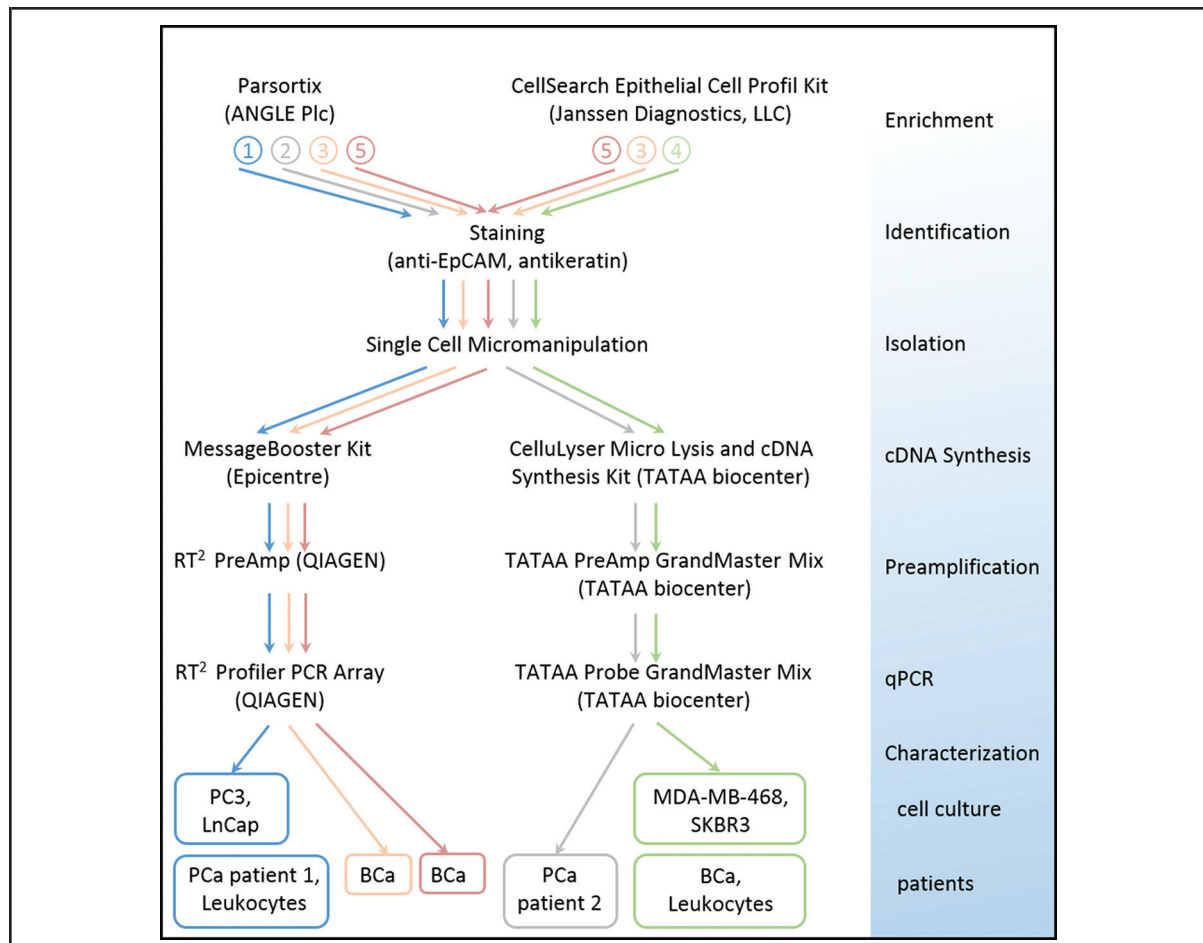


Fig. 1. Methodological workflow of single tumor cell RNA profiling.

To enrich tumor cells from spiking samples or CTCs out of clinical samples, the CellSearch Epithelial Cell Profile Kit (Janssen Diagnostics) or the Parsortix system (ANGLE Plc) was used. After tumor cell enrichment, the cells were identified using an EpCAM/pan-keratin-based staining protocol followed by micromanipulation, cDNA synthesis, preamplification, and qPCR. The different numbers and colored lines illustrate individual workflows of sample processing.

MULTIMARKER EXPRESSION PROFILING OF SINGLE CELLS

TATAA PreAMP and qPCR. To analyze a multimarker profile of single cells, cells were lysed using the CelluLyser Micro Kit. cDNA was produced using the GrandScript cDNA Synthesis Kit and was subsequently preamplified with the CTC GrandPerformance assays using the PreAmp GrandMaster[®] Mix (TATAA Biocenter). PCR was done according to the manufacturer's instructions using the Bio-Rad CFX96 cycler (Bio-Rad).

RT² PreAMP and RT² Profiler PCR Array. The Message Booster Kit[™] was applied in combination with the RT² PreAMP Kit (QIAGEN) and different RT² Profiler PCR Arrays (Human Breast Cancer, Prostate Cancer, or EMT PCR Array or Cancer Inflammation & Immunity Cross-talk PCR Array, QIAGEN). PCR was done according to

the manufacturer's instructions using the Bio-Rad CFX96 cycler (Bio-Rad).

SINGLE CELL qPCR DATA ANALYSIS

Single cell qPCR data were generated as illustrated in Fig. 1. Quantification cycle (C_q) values above 35 were treated as "off-scale data." All missing data points were also treated as "off-scale data" and replaced with a C_q value of 37. This was 2 cycles above the cutoff, which was considered giving a balanced weight to the negative observation of transcripts in individual cells (12). The C_q values were converted to relative quantities and transformed to log base 2 scale. The expression data were not normalized to any endogenous markers because of the stochasticity of single cell expression (13). The measured cDNA concentrations, which are proportional to mRNA concentra-

tions (14), are thus expressed per cell. To display all data together, principal component analysis (PCA) and hierarchical clustering were used. Each method used a different mathematical approach to separate samples into groups. PCA reduced multidimensional data into 2-dimensional charts with small loss of information. Each point in the PCA graph contained information about the expression of all the genes. For the hierarchical clustering and PCA analyses, data were mean centered to reduce the influence of the variable overall expression level of the genes (15).

PATIENT SAMPLES

Analysis of human samples was carried out in accordance with the guidelines for experimentation with humans by the Chambers of Physicians of the State of Hamburg ("Hamburger Ärztekammer"). Written informed consent was obtained from all patients and the experiments conformed to the principles set out in the World Medical Association (WMA) Declaration of Helsinki and the Department of Health and Human Services Belmont Report. Breast cancer samples were obtained from the Department of Gynecology, University Medical Center Hamburg-Eppendorf, Germany. Prostate cancer samples were collected at the Practice Hematology and Oncology, Hamburg, Germany. All blood samples were collected into EDTA tubes (7.5 mL) and processed within 4 h after blood withdrawal.

Results

VALIDATION OF SINGLE CELL RNA ANALYSIS

Four different kits were tested for single cell RNA analysis: the NucleoSpin RNA II Kit[®] (Macherey-Nagel); the PicoPure RNA Isolation Kit[®] (Life Technologies); the MessageBooster Kit (Epicentre); and the CelluLyser Micro Kit and cDNA Synthesis Kit (TATAA Biocenter). To verify the kits, 1, 5, 10, and 50 MDA-468 or the SKBR3 cells were directly spiked into lysis buffer followed by qualitative PCR amplifying *EpCAM*, *EGFR*, *ERBB2*, *KRT19*, and *ACTB* transcripts. Only the MessageBooster Kit and the CelluLyser Micro and cDNA Synthesis Kit produced consistent RNA profiles of the tested cell lines down to single cell level (see online Supplemental Fig. 1). Hence, these kits were used for further studies.

We had to establish a specific staining protocol that was compatible with downstream single cell profiling to distinguish CTCs from leukocytes in clinical samples. In our study, EpCAM and pan-keratins were used as target proteins for tumor cell identification (Fig. 2 A and online Supplemental Fig. 2A).

Having established a reliable staining protocol, single breast (MDA-468 and SKBR3; n = 3) or prostate cancer cells (LnCap and PC3; n = 3) were spiked into 7.5 mL EDTA blood of healthy donors (n = 2) and pro-

cessed by CellSearch or Parsortix. Next, tumor cells or remaining leukocytes were isolated and analyzed using either the RT² PreAmp and Profiler Human Prostate Cancer PCR Array (QIAGEN) or the TATAA PreAmp GrandMaster[®] Mix and TATAA Probe GrandMaster[®] Mix (TATAA Biocenter) (Fig. 1, blue arrow and green arrow).

Tumor cells could clearly be discriminated from leukocytes based on their expression profiles (Fig. 2, B and C). All details of the measured Cq values are listed in online Supplemental Tables 1 and 2.

QUALITATIVE PCR AS INDICATOR FOR THE SUCCESS OF FURTHER MULTIMARKER PROFILING

For clinical samples, the criteria for a cell to be classified as CTC were: intact morphology (bright field microscopy), nucleus larger than 4 μm in diameter, and positive staining for EpCAM and/or pan-keratins (Supplemental Fig. 2A). The *KRT19* transcripts have been widely used to identify and study CTCs in cancer patients (5, 6). Hence, we decided to use this marker as an additional "CTC indicator" by qualitative PCR before in-depth multimarker qPCR analysis. In total, 55 single CTCs from 5 different donors were analyzed in our study. However, reliable multimarker analysis was only possible when intense signals for *KRT19* were observed (n = 39). Thus, we would recommend performing additional "qualitative PCR" tests as quality control before single cell multimarker analyses in future studies (Fig. 1 and online Supplemental Fig. 2B).

ACCESSION OF TUMOR HETEROGENEITY BY MULTIPLEX TRANSCRIPTOME PROFILING

In-depth analysis of CTCs from a patient with breast cancer (enriched by CellSearch) revealed that RNA expression profiles of CTCs could clearly be discriminated from leukocytes (Fig. 3, A and B, and Fig. 1, green arrows). Genes such as *EpCAM*, cadherin 1_1 (*CDH1_1*), secretoglobulin family 2A member 1 (*SCGB2A1*)/*MAM*, estrogen receptor 1 (*ESR1*), epithelial membrane protein 2 (*EMP2*), and *KRT19* were exclusively expressed in CTCs, while protein tyrosine phosphatase, receptor type C (*PTPRC*; formerly called *CD45*) and vimentin (*VIM*) were predominant in the leukocytes. Although CTCs could clearly be distinguished from the leukocytes, 2 CTCs were positive for both, the epithelial transcripts (*EpCAM* and *KRT19*) and the leukocyte/mesenchymal markers (*CD45* and *VIM*).

Principle component analysis (PCA) of the expression profiles - measured for the individual CTCs from this patient - indicated that there might be 2 clusters, suggesting 2 CTC subtypes (Fig. 3, C-E). One CTC, which had substantially lower overall transcript levels than the other cells, separated from the 2 CTC clusters and from the leukocytes, indicating it was a deviant possibly due to damage during processing (Fig. 3, A-D). Genes significantly differentially

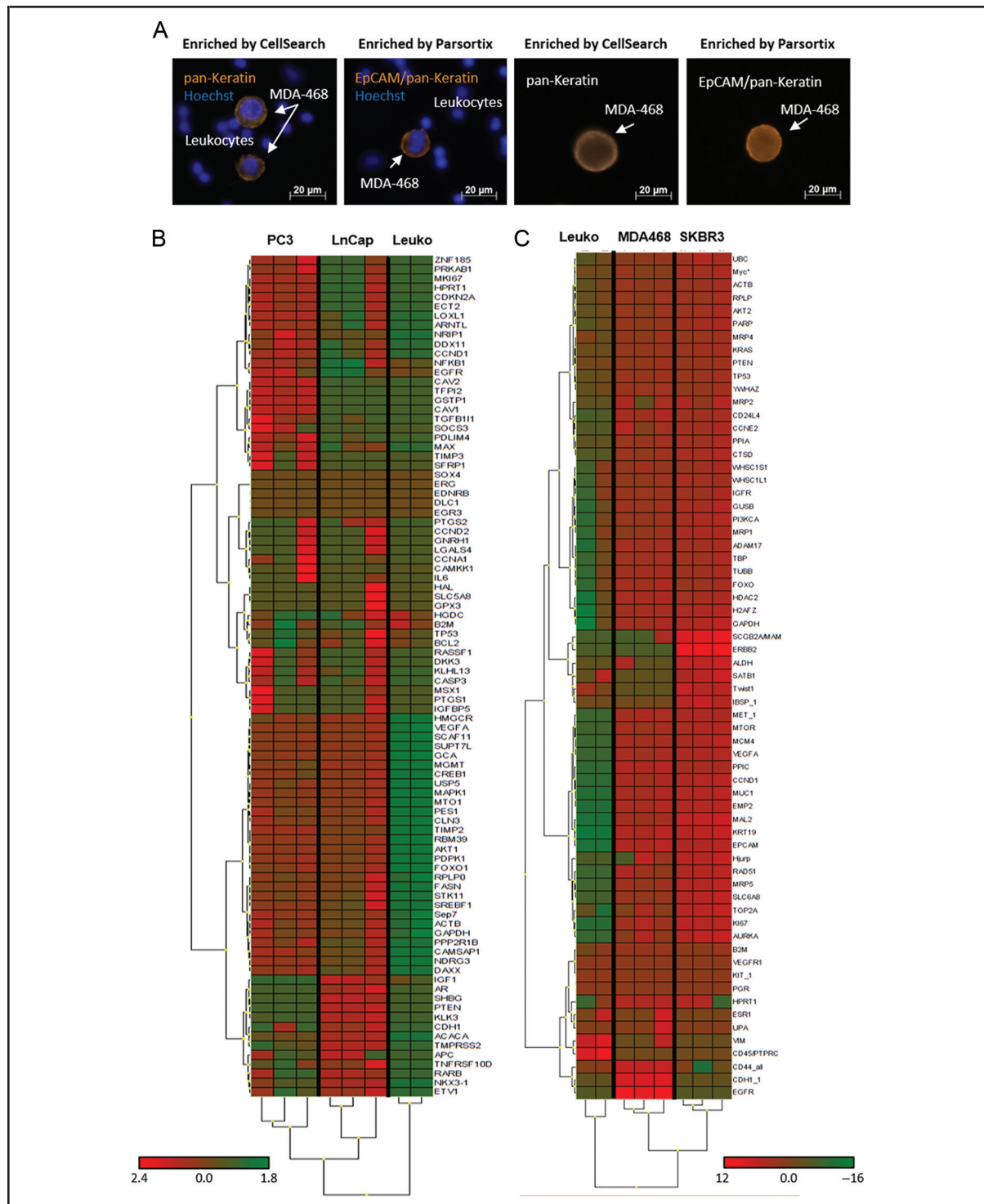


Fig. 2. Single cell RNA analysis of EpCAM and/or pan-keratin stained cell culture cells and leukocytes.

(A), Cells were enriched by CellSearch or Parsortix and processed as described in Fig. 1. (B), Staining of the tumor cells after enrichment. (C), Dendrogram and heat map analyses of prostate and breast cancer cells after staining [LnCap, PC3, MDA-468, and SKBR3 (n = 3 per cell line)] and single leukocytes from healthy individuals (n = 2). Data are mean centered, with mean expression responses to zero. Red and green colors represent up- and downregulation, respectively (see scale), relative to the mean of the pool.

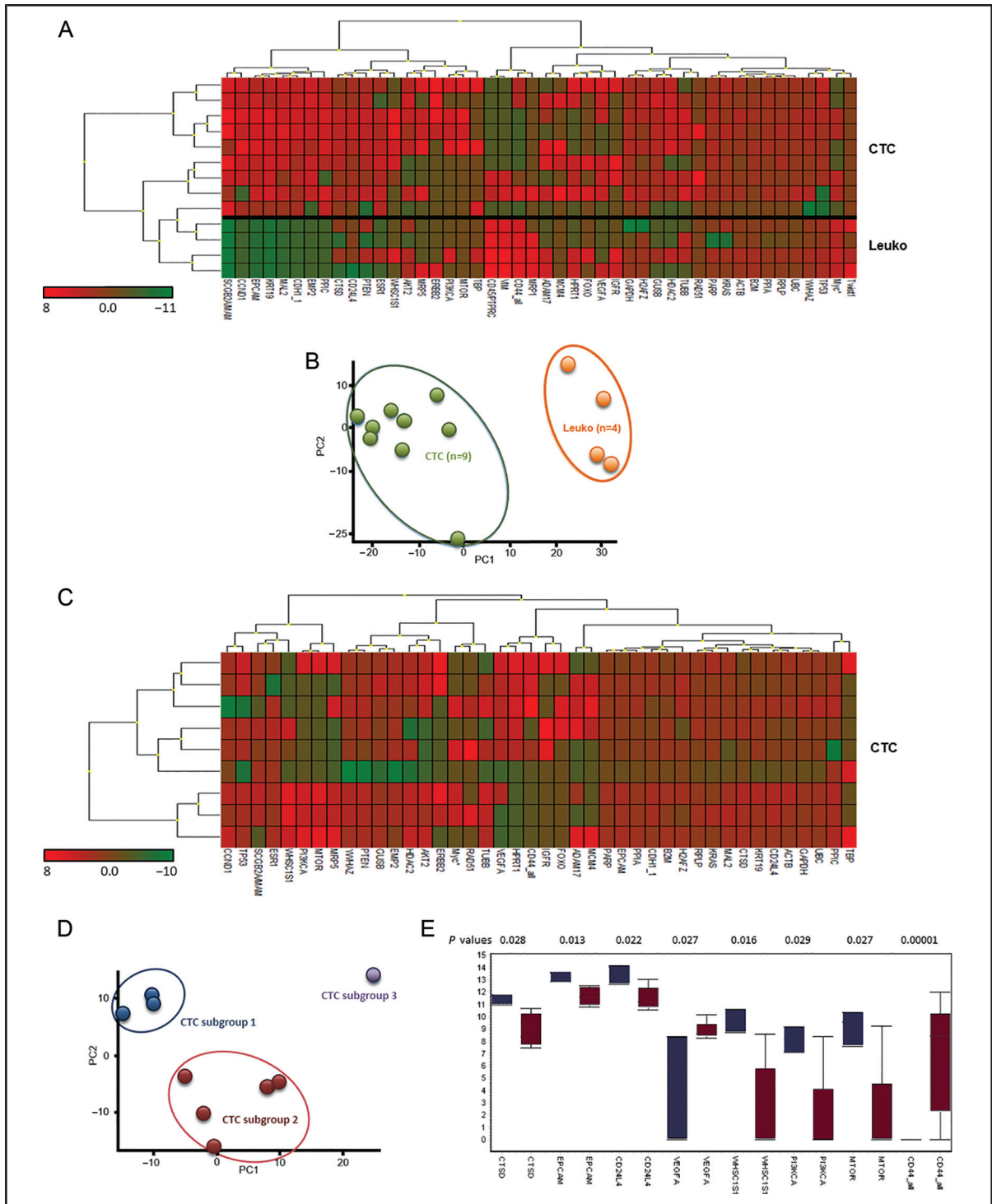


Fig. 3. Molecular signature of CTCs and leukocytes from a breast cancer patient.

Gene-expression profile of CTCs (n = 9) and leukocytes (n = 2) enriched by CellSearch and analyzed using the CelluLyser Micro and cDNA Synthesis Kit together with the GrandPerformance panel. (A), Dendrogram and heat map presenting hierarchical clustering analysis of CTCs and leukocytes. (B), PCA classifying the CTCs and leukocytes. (C), Dendrogram and heatmap of CTCs only. (D), PCA and hierarchical clustering of CTCs subgroups. (E), Box plot showing the genes that display significantly different expression profiles between subgroup 1 and 2 of CTCs.

expressed between the 2 CTC subgroups are shown in Fig. 3E. CTCs in subgroup 1 displayed increased transcription of genes involved in cell growth and tumor proliferation [phosphatidylinositol-4,5-bisphosphate 3-kinase catalytic subunit alpha (*PIK3CA*) and mechanistic target of rapamycin (*MTOR*)]. These cells furthermore showed low expression levels of the stem cell marker CD44 molecule (Indian blood group; *CD44*) and high expression levels for Wolf-Hirschhorn syndrome candidate 1 (*Whsc1*), a gene encoding for histone methyltransferase NSD2 known to play an important role in cancer proliferation, survival, and tumor growth (16). Detailed expression profiles (Cq values) of all CTCs from this patient are summarized in online Supplemental Table 3.

Thirteen additional CTCs from another breast cancer patient, enriched in parallel by Parsortix (n = 7 CTCs) and CellSearch (n = 6 CTCs), could be processed by targeting EMT-specific transcripts (Fig. 4, A–C, and Fig. 1, red arrows). Again, single cell CTC subpopulations could be identified depending on the expression profile but independently of the enrichment strategy (Fig. 4 B). The most important genes clustering CTCs in the subgroups were cadherin 2 (*CDH2*), collagen type I alpha 2 chain (*COL1A2*), collagen type V alpha 2 chain (*COL5A2*), fibronectin 1 (*FNI*), microtubule associated protein 1B (*MAP1B*), matrix metalloproteinase 3 (*MMP3*), SRY-box 10 (*SOX10*), secreted phosphoprotein 1 (*SPP1*), zinc finger E-box binding homeobox 1 (*ZEB1*), and zinc finger E-box binding homeobox 1 (*ZEB2*; Fig. 4C).

CTCs from a patient with prostate cancer (n = 8) (enriched by Parsortix only) could also be clustered into different subgroups based on their expression profiles (Fig. 5, A–C, and Fig. 1, blue arrow). Only genes with transcripts detected in at least 3 of the CTCs were considered for PCA. The most important genes distinguishing CTCs into the subgroups were vascular endothelial growth factor A (*VEGFA*; a marker that stimulates vasculogenesis and angiogenesis also relevant as therapeutic target) (17), AR (a receptor that plays a key role in the development and progression of PC and is used as therapeutic target) (18), nuclear factor κ B (*NF- κ B*; a transcription factor known to regulate AR expression and PC growth) (19), NK3 homeobox 1 (*NKX3-1*; an androgen-regulated transcription factor believed to act as a suppressor of the pathogenic ERG, ETS transcription factor (*TMPRSS2-ERG* rearrangement) (20), and transmembrane protease, serine 2 (*TMPRSS2*; an androgen-regulated protease known to be contributing to regulation of cancer growth) (20) (Fig. 5C). Cq values of all CTCs from this patient are summarized in online Supplemental Table 4.

CTC subgroups (enriched by Parsortix) were also present in an additional sample from another patient with prostate cancer (Fig. 6, A–C, and Fig. 1, gray ar-

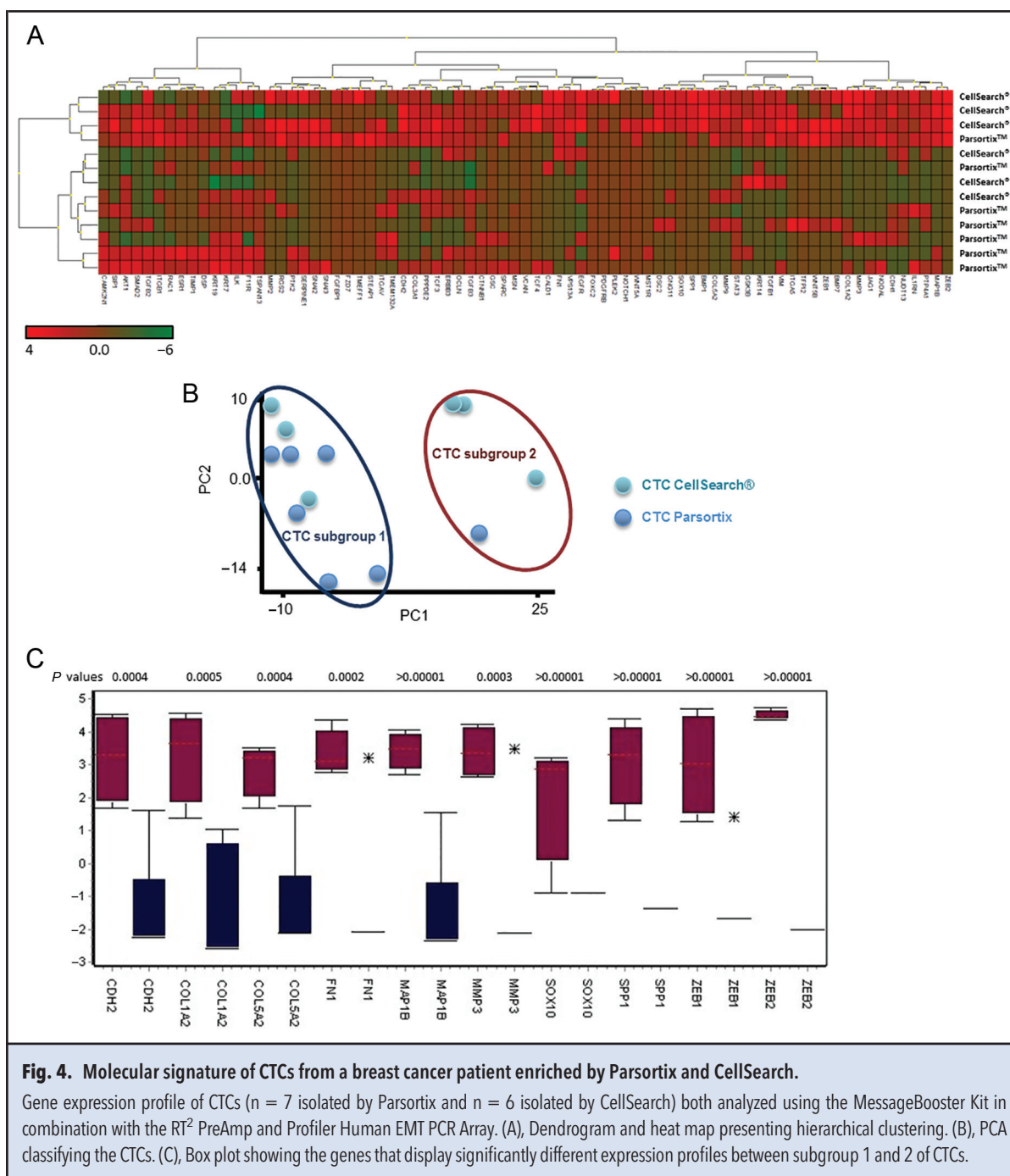
row). CTCs in one of the subgroups showed increased expression levels of RAD51 recombinase (*RAD51*). Overexpression of this marker has been associated with aggressive prostate cancer (21). CTCs in the other subgroup displayed high expression of markers discussed to be relevant for supporting therapeutic decisions in prostate cancer [androgen receptor V7 (*AR-V7*) and signal transducer and activator of transcription 3 (*STAT3*)] (4, 22). Summarized Cq values of CTCs from this patient are listed in online Supplemental Table 5.

ACTIVATION OF INFLAMMATION AND IMMUNITY SIGNALING IN CTCs

Lively debate is ongoing about communication between tumor cells and the cellular mediators of inflammation and immunity (23). Thus, we also decided to analyze the expression of genes involved in cancer inflammation and immune cross talk (Fig. 1, orange arrow). Here, both CellSearch and Parsortix enrichment strategies were applied to 2 blood samples from the same patient. The enrichment method did not bias expression of the reference genes included in the analysis (mean Cq after CellSearch enrichment: 25.31 vs mean Cq after Parsortix: 25.16), demonstrating consistent workflows of the 2 enrichment strategies. In this case, several genes involved in cross talks between immune cells and cancer cells, such as C-C motif chemokine ligand 4 (*CCL4*), C-X-C motif chemokine ligand 2 (*CXCL2*), *CXCL9*, interleukin 15 (*IL15*), *IL1B*, or *IL8* showed different expression levels between the individual CTCs captured via EpCAM or by size (see online Supplemental Fig. 3 and online Supplemental Table 6). It is notable that tumor cell–derived *CCL4* protein, which was one of the identified markers, can promote bone metastasis by interacting with CCR5-expressing nontumor cells (24). Chemokines have an important role in cancer metastasis and might mediate a signaling network that links metastasis formation and chemotherapy resistance. Chemokines, including *CXCL2*, *CXCL8* (*IL8*), showed substantially higher expression in CTCs enriched with the Parsortix system. In relation to this observation, enhanced *IL15* expression has previously been detected in colorectal cancer cells and shown to play an important role in cell proliferation, invasion, and metastasis formation (25). In our study, *IL15* transcript levels showed large variations across CTCs independently of enrichment strategy.

Discussion

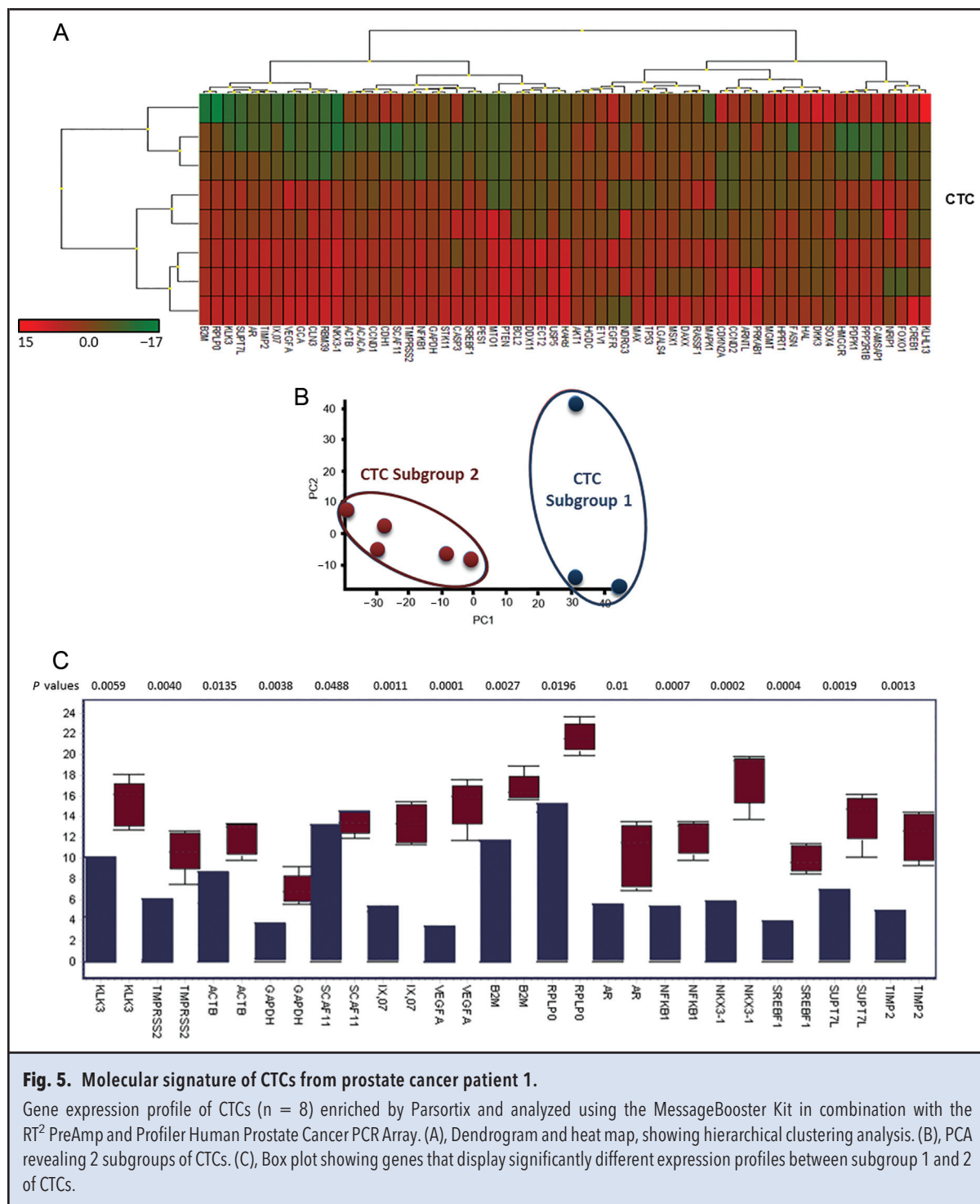
We developed optimized workflows for robust enrichment and transcriptomic profiling of single CTCs. Enrichment of CTCs was performed with 2 different platforms: the EpCAM-dependent CellSearch system



(approved by the US Food and Drug Administration) and a novel, marker-independent size-based approach (Parsortix) (11). Our workflows allow for the characterization of different CTC single cell subpopulations depending on the markers used for the identification.

Our single cell data showed high detection rates of the targeted transcripts. The GrandPerformance assays are probe based, thus avoiding false positive results due

to formation of primer dimers and other aberrant products, while the RT² Profiler assays are SYBR based and generate signal also from aberrant PCR products. This is, however, minimized by careful assay optimization and by rejecting Cq values ≥ 35 . Expression of reference genes cannot be used for normalization of single cell data due to the underlying burst kinetics (26), but their overall expression level can serve as a



quality indicator. CTCs with exceedingly low transcript levels of reference genes are likely to have been damaged during the processing.

We found a minor subpopulation of epithelial marker-positive (e.g., *KRT19* and *EpCAM*) and *CD45*-

positive cells in clinical samples (Fig. 3). These cells were also strongly positive for markers such as twist family bHLH transcription factor (*Twist*), *CD44*, ATP binding cassette subfamily C member 1 (*ABCC1*), or ADAM metallopeptidase domain 17 (*ADAM17*). We assume

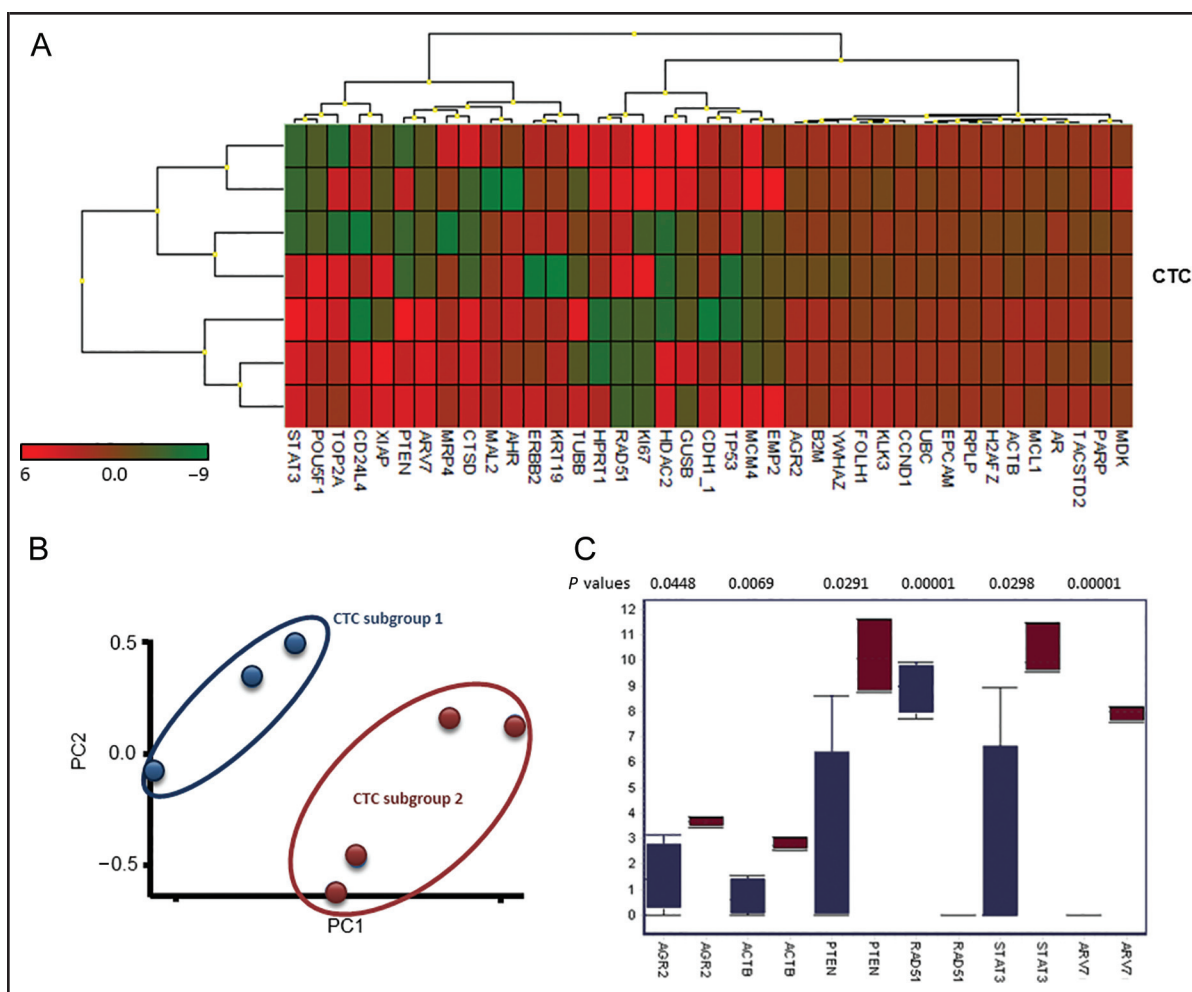


Fig. 6. Molecular signature of CTCs from prostate cancer patient 2.

Gene expression profile of CTCs ($n = 7$) enriched by Parsortix system and analyzed using the CelluLyser Micro and cDNA Synthesis Kit together with the GrandPerformance panel. (A), Dendrogram and heat map, showing hierarchical clustering analysis. (B), PCA revealing 2 subgroups of CTCs. (C), Box plot showing genes that display significantly different expression profiles between subgroup 1 and 2 of CTCs.

that these cells are tumor cells but the role of *CD45*-positive CTCs is not clear yet (27, 28). Thus, our assay might help to identify the relevance of this specific cell type in future studies.

Focusing on the transcript signatures of CTCs, different subgroups were identified in individual patients (independently of the enrichment strategy (see online Supplemental Fig. 4 A – C). These subgroups were characterized by divergent expression of, e.g., EMT-associated genes (*CDH2*, *COL1A2*, *COL5A2*, *FN1*, *MAP1B*, *MMP3*, *SOX10*, *SPP1*, *ZEB1*, and *ZEB2*), DNA repair genes (*RAD51*) (21) or targets relevant for cancer therapy. For example, *EGFR* or *ERBB2*-specific transcripts were frequently present in CTCs (Figs. 4–6). *ERBB2* is an effective target in breast cancer and further-

more discussed to play also an important role in PC (29, 30). Here, *ERBB2* transcripts were present in PC-derived CTCs (see online Supplemental Fig. 6). Controlling the *ERBB2* pathway could be an attractive combinational therapeutic approach together with second-generation antiandrogen agents such as enzalutamide and abiraterone acetate to remove castration-resistant prostate cancer (30). We also show that *ERBB2*-positive CTCs might express *AR-V7* (3 out of 7 CTCs in the same patient) (Fig. 6). *AR-V7*, a constitutively active splice variant of the AR detected in CTC pools, was recently found to drive castration-resistant growth and resistance to enzalutamide from patients with metastatic in castration-resistant prostate cancer (4). Thus, we demonstrate the differential expression of *ERBB2* and/or

AR-V7 between subgroups of CTCs in an individual patient with prostate cancer, indicating that unraveling the transcriptome of CTCs might help to monitor the emergence of driver molecules for resistance and thereby unveil patients who would profit from optional therapies, e.g., using galeterone instead of enzalutamide and abiraterone (plus ERBB2 inhibitors).

In addition, transcripts that have been reported to be relevant for metastatic processes (EpCAM, CD44, CD24) or potential drug targets (mTOR, PI3K, VEGFA) (31–33) were also found to be significantly differently expressed among breast cancer-derived CTCs (Fig. 3). Previous reports suggested the existence of tumor stem cells that are characterized by upregulation of CD44 and the downregulation of CD24 (34). However, the role of CD24 remains controversial since both CD44^{high}/CD24^{low} and CD44^{high}/CD24^{high} cells have been shown to initiate tumor growth (35, 36). In the present study, CD44 emerged as an allocation factor between 2 subgroups of CTCs derived from the same breast cancer patient, whereas CD24 was marginally altered between the same subgroups. Interestingly, the CD44^{low}/CD24^{high} subgroup showed high expression levels of *PI3K* and *MTOR*. The PI3K/AKT/mTOR signaling cascade is one of the most important intracellular pathways in cancer cells (37). Numerous efforts have been made to develop targeted therapies inhibiting this cascade in hormone receptor positive, ERBB2-negative breast cancer in combination with hormonal therapy (38).

Emerging data suggests that the heterogeneity of cancer thought to be causative for the functional plasticity necessary for tumor cells to evade therapeutic approaches, as well as prosperous adoption to foreign microenvironments within the metastatic niche, is driven by transcriptional changes (39). Understanding this heterogeneity with the presented workflow allows for a better understanding of the mechanisms involved in cancer progression. RNA analysis of CTCs offers the opportunity to stratify patients with metastatic disease into phenotypical subgroups according to their expression profiles, providing an important framework for therapeutic decisions based on a simple blood test (“liquid biopsy”) (1, 28). Such information is expected to be most valuable in the selection of personalized therapies, since the most active pathways are critical for the particular CTCs present and may be their Achilles heel if suitable drugs targeting that pathway are available. Particularly when combined with mutational profiling, which reveals any crit-

ical mutations affecting the sensitivity for targeted therapy (2, 3), it might support decision-making for individualized treatments.

In summary, we established reliable workflows to study multimarker profiles of single CTCs by low cost qPCR approaches. In principle, these workflows can be combined with any CTC enrichment system that enables isolation of high quality RNA. Thus, these workflows could become a valuable new tool in biomedical research. Although the number of patients/CTCs studied in this proof-of-principle study was small, multivariate analysis of expression profiles indicated that subgroups of CTCs with different phenotypes are present within each CTC-positive patient. Inpatient heterogeneity of CTCs might contribute to resistance to therapy. This hypothesis has to be tested in future clinical studies.

Author Contributions: All authors confirmed they have contributed to the intellectual content of this paper and have met the following 3 requirements: (a) significant contributions to the conception and design, acquisition of data, or analysis and interpretation of data; (b) drafting or revising the article for intellectual content; and (c) final approval of the published article.

Authors' Disclosures or Potential Conflicts of Interest: Upon manuscript submission, all authors completed the author disclosure form. Disclosures and/or potential conflicts of interest:

Employment or Leadership: M. Kubista, TATAA Biocenter.

Consultant or Advisory Role: None declared.

Stock Ownership: V. Novosadova, TATAA Biocenter; M. Kubista, TATAA Biocenter.

Honoraria: None declared.

Research Funding: Grant P303-16-10214S, Grant Agency of the Czech Republic, project BIOCEV CZ.1.05/1.1.00/02.0109 provided by ERDF and MEYS, and project BIOCEV-FAR LQ1604 NPU II provided by MEYS. T.M Gorges, S. Riethdorf, and K. Patel, City of Hamburg, Landesexzellenzinitiative Hamburg (LEXI 2012; Tumor targeting via cell surface molecules essential in cancer progression and dissemination), and ERC Advanced Investigator Grant DISSECT, TRANSCAN ERA-Network: Grant CTC-SCAN; T. M. Gorges and K. Patel, Innovative Medicines Initiative Joint Undertaking under grant agreement no. 115749, resources of which are composed of financial contribution from the European Union's Seventh Framework Programme (FP7/2007-2013) and EFPIA companies.

Expert Testimony: None declared.

Patents: None declared.

Role of Sponsor: The funding organizations played no role in the design of study, choice of enrolled patients, review and interpretation of data, and final approval of manuscript.

Acknowledgments: The authors thank all patients and their families.

References

- Gorges TM, Pantel K. Circulating tumor cells as therapy-related biomarkers in cancer patients. *Cancer Immunol Immunother* 2013;62:931–9.
- Gasch C, Bauernhofer T, Pichler M, Langer-Freitag S, Reeh M, Seifert AM, et al. Heterogeneity of epidermal growth factor receptor status and mutations of KRAS/PIK3CA in circulating tumor cells of patients with colorectal cancer. *Clin Chem* 2013;59:252–60.
- Heitzer E, Auer M, Gasch C, Pichler M, Ulz P, Hoffmann EM, et al. Complex tumor genomes inferred from single circulating tumor cells by array-CGH and next-generation sequencing. *Cancer Res* 2013;73:2965–75.
- Antonarakis ES, Lu C, Wang H, Lubner B, Nakazawa M, Roeser JC, et al. Ar-v7 and resistance to enzalutamide and abiraterone in prostate cancer. *N Engl J Med* 2014; 371:1028–38.
- Stathopoulou A, Angelopoulou K, Perraki M, Georgoulas V, Malamos N, Lianidou E. Quantitative rt-pcr luminescent hybridization assay with an RNA internal standard for cytokeratin-19 mRNA in peripheral blood of patients with breast cancer. *Clin Biochem* 2001;34:

- 651–9.
6. Stathopoulou A, Gizi A, Perraki M, Apostolaki S, Malamos N, Mavroudis D, et al. Real-time quantification of ck-19 mRNA-positive cells in peripheral blood of breast cancer patients using the lightcycler system. *Clin Cancer Res* 2003;9:5145–51.
 7. Kasimir-Bauer S, Hoffmann O, Wallwiener D, Kimmig R, Fehm T. Expression of stem cell and epithelial-mesenchymal transition markers in primary breast cancer patients with circulating tumor cells. *Breast Cancer Res* 2012;14:R15.
 8. Vaiopoulos AG, Kostakis ID, Gkioka E, Athanasoula K, Pikoulis E, Papalambros A, et al. Detection of circulating tumor cells in colorectal and gastric cancer using a multiplex PCR assay. *Anticancer Res* 2014;34:3083–92.
 9. Yu M, Bardia A, Wittner BS, Stott SL, Smas ME, Ting DT, et al. Circulating breast tumor cells exhibit dynamic changes in epithelial and mesenchymal composition. *Science* 2013;339:580–4.
 10. Ozkumur E, Shah AM, Ciciliano JC, Emmink BL, Miyamoto DT, Brachtel E, et al. Inertial focusing for tumor antigen-dependent and -independent sorting of rare circulating tumor cells. *Sci Transl Med* 2013;5:179ra47.
 11. Hvichia GE, Parveen Z, Wagner C, Janning M, Quidde J, Stein A, et al. A novel microfluidic platform for size and deformability based separation and the subsequent molecular characterization of viable circulating tumor cells. *Int J Cancer* 2016;138:2894–904.
 12. Stahlberg A, Rusnakova V, Forootan A, Anderova M, Kubista M. RT-qPCR workflow for single-cell data analysis. *Methods* 2013;59:80–8.
 13. Bengtsson M, Stahlberg A, Rorsman P, Kubista M. Gene expression profiling in single cells from the pancreatic islets of Langerhans reveals lognormal distribution of mRNA levels. *Genome Res* 2005;15:1388–92.
 14. Stahlberg A, Hakansson J, Xian X, Semb H, Kubista M. Properties of the reverse transcription reaction in mRNA quantification. *Clin Chem* 2004;50:509–15.
 15. Bergkvist A, Rusnakova V, Sindelka R, Garda JM, Sjogreen B, Lindh D, et al. Gene expression profiling: clusters of possibilities. *Methods* 2010;50:323–35.
 16. Yang P, Guo L, Duan ZJ, Tepper CG, Xue L, Chen X, et al. Histone methyltransferase NSD2/MMSET mediates constitutive NF-kappaB signaling for cancer cell proliferation, survival, and tumor growth via a feed-forward loop. *Mol Cell Biol* 2012;32:3121–31.
 17. Welti J, Loges S, Dimmeler S, Carmeliet P. Recent molecular discoveries in angiogenesis and antiangiogenic therapies in cancer. *J Clin Invest* 2013;123:3190–200.
 18. Anantharaman A, Friedlander TW. Targeting the androgen receptor in metastatic castrate-resistant prostate cancer: a review. *Urol Oncol* 2016;34:356–67.
 19. Zhang L, Altuwajri S, Deng F, Chen L, Lal P, Bhanot UK, et al. NF-KappaB regulates androgen receptor expression and prostate cancer growth. *Am J Pathol* 2009;175:489–99.
 20. Bowen C, Zheng T, Gelman EP. Nkx3.1 suppresses tmprss2-erg gene rearrangement and mediates repair of androgen receptor-induced DNA damage. *Cancer Res* 2015;75:2686–98.
 21. Mitra A, Jameson C, Barbachano Y, Sanchez L, Kote-Jarai Z, Peock S, et al. Overexpression of RAD51 occurs in aggressive prostatic cancer. *Histopathology* 2009;55:696–704.
 22. Bosch-Barrera J, Menendez JA. Silibinin and STAT3: a natural way of targeting transcription factors for cancer therapy. *Cancer Treat Rev* 2015;41:540–6.
 23. Schreiber RD, Old LJ, Smyth MJ. Cancer immunoeediting: integrating immunity's roles in cancer suppression and promotion. *Science* 2011;331:1565–70.
 24. Mukaida N, Sasaki S, Baba T. Id: 33: CCL4 can promote bone metastasis of a murine breast cancer cell line, by interacting CCR5-expressing non-tumor cells in bone marrow. *Cytokine* 2015;76:70.
 25. Kuniyasu H, Oue N, Nakae D, Tsutsumi M, Denda A, Tsujiuchi T, et al. Interleukin-15 expression is associated with malignant potential in colon cancer cells. *Pathobiology* 2001;69:86–95.
 26. Kumar N, Singh A, Kulkarni RV. Transcriptional bursting in gene expression: analytical results for general stochastic models. *PLoS Comput Biol* 2015;11:e1004292.
 27. Yu M, Stott S, Toner M, Maheswaran S, Haber DA. Circulating tumor cells: approaches to isolation and characterization. *J Cell Biol* 2011;192:373–82.
 28. Alix-Panabieres C, Pantel K. Challenges in circulating tumor cell research. *Nat Rev Cancer* 2014;14:623–31.
 29. Riethdorf S, Muller V, Zhang L, Rau T, Loibl S, Komor M, et al. Detection and HER2 expression of circulating tumor cells: prospective monitoring in breast cancer patients treated in the neoadjuvant GeparQuattro trial. *Clin Cancer Res* 2010;16:2634–45.
 30. Muniyan S, Chen SJ, Lin FF, Wang Z, Mehta PP, Batra SK, Lin MF. ErbB-2 signaling plays a critical role in regulating androgen-sensitive and castration-resistant androgen receptor-positive prostate cancer cells. *Cell Signal* 2015;27:2261–71.
 31. Johnston SR. Enhancing endocrine therapy for hormone receptor-positive advanced breast cancer: cotargeting signaling pathways. *J Natl Cancer Inst* 2015;107.
 32. Nagaraj G, Ma C. Revisiting the estrogen receptor pathway and its role in endocrine therapy for postmenopausal women with estrogen receptor-positive metastatic breast cancer. *Breast Cancer Res Treat* 2015;150:231–42.
 33. Kristensen TB, Knutsson ML, Wehland M, Laursen BE, Grimm D, Warnke E, Magnusson NE. Antivascular endothelial growth factor therapy in breast cancer. *Int J Mol Sci* 2014;15:23024–41.
 34. Clarke MF, Dick JE, Dirks PB, Eaves CJ, Jamieson CH, Jones DL, et al. Cancer stem cells—perspectives on current status and future directions: AACR Workshop on cancer stem cells. *Cancer Res* 2006;66:9339–44.
 35. Jaggupilli A, Elkord E. Significance of CD44 and CD24 as cancer stem cell markers: an enduring ambiguity. *Clin Dev Immunol* 2012;2012:708036.
 36. Yeung TM, Gandhi SC, Wilding JL, Muschel R, Bodmer WF. Cancer stem cells from colorectal cancer-derived cell lines. *Proc Natl Acad Sci USA* 2010;107:3722–7.
 37. Wu P, Liu T, Hu Y. PI3K inhibitors for cancer therapy: what has been achieved so far? *Curr Med Chem* 2009;16:916–30.
 38. Baselga J, Campone M, Piccart M, Burris HA, 3rd, Rugo HS, Sahmoud T, et al. Everolimus in postmenopausal hormone-receptor-positive advanced breast cancer. *N Engl J Med* 2012;366:520–9.
 39. Chen J, Weiss WA. Alternative splicing in cancer: implications for biology and therapy. *Oncogene* 2015;34:1–14.

Supplement Table 1: Expression profile of prostate cancer cell lines and leukocytes

	PC3_1	PC3_2	PC3_3	LnCap_1	LnCap_2	LnCap_3	Leuko_1	Leuko_2
ACACA	30,72	29,33	30,22	24,26	24,25	23,64	N/A	39,19
AKT1	27,85	28,75	28,22	29,31	29,75	26,88	37,8	39,21
APC	27,31	N/A	34,84	24,95	25,16	35,62	35,91	35,54
AR	N/A	N/A	N/A	32,24	31,29	28,75	N/A	40,39
ARNTL	23,73	26,54	25,76	31,91	N/A	23,43	36,9	N/A
BCL2	33,42	35,51	32,6	31,66	34,22	28,72	32,25	33,66
CAMKK1	N/A	N/A	33,23	N/A	N/A	36,49	N/A	N/A
CAMSAP1	23,29	23,35	26,36	28,45	28,82	22,92	N/A	N/A
CASP3	25,54	37,48	23,85	N/A	33,25	22,38	N/A	N/A
CAV1	20,1	22,27	21,08	N/A	N/A	N/A	N/A	N/A
CAV2	24,5	25,97	24,03	38,13	38,22	34,78	N/A	N/A
CCNA1	32,07	N/A	25,01	N/A	38,04	34,25	N/A	N/A
CCND1	27,39	25,52	28,3	39,24	33,5	26,88	38,76	N/A
CCND2	N/A	38,91	32,41	39,58	N/A	31,29	38,27	39,4
CDH1	N/A	26,12	N/A	27,28	27,81	23,7	37,71	N/A
CDKN2A	21,03	24,66	22,17	N/A	N/A	21,93	N/A	N/A
CLN3	24,23	26,96	27,4	26,83	27,14	23,83	N/A	N/A
CREB1	24,44	24,52	28,26	24,79	25,08	22,02	37,26	N/A
DAXX	29,13	29,15	27,82	32,57	31,45	26,67	N/A	N/A
DDX11	29,27	24,74	26,22	N/A	33,02	27,06	40,3	N/A
DKK3	32,38	36,68	34,47	35,13	36,98	33,16	37,67	39,37
DLC1	N/A	39,28	39,33	38,67	N/A	37,84	N/A	N/A
ECT2	21,36	25,69	23,77	37,75	38,26	22,02	40,68	39,14
EDNRB	35,1	N/A	N/A	N/A	37,22	N/A	N/A	N/A
EGFR	28,22	27,52	32,71	40,54	37,14	31,77	31,9	32,58
EGR3	39,38	40,8	38,21	38,08	N/A	38,12	N/A	N/A
ERG	37,03	38,25	37,68	N/A	N/A	36,49	N/A	N/A
ETV1	25,15	36,54	32,53	24,67	24,84	20,08	N/A	N/A
FASN	29,28	29,28	28,39	29,47	30,22	24,7	N/A	N/A
FOXO1	29,72	29,3	27,35	29,31	29,51	27,25	39,38	N/A
GCA	24,03	23,35	23,29	23,55	23,89	21,9	36,79	37,55
GNRH1	N/A	N/A	25,87	N/A	N/A	26,56	N/A	N/A
GPX3	39,44	35,7	37,38	N/A	N/A	34,13	36,16	36,4
GSTP1	19,89	21,14	20,2	N/A	N/A	35,8	35,02	35,98
HAL	38,73	N/A	N/A	N/A	N/A	34,89	N/A	N/A
HMGCR	27,95	24,15	25,78	23,9	24,29	22,38	39,26	N/A
IGF1	N/A	39,53	40,27	23,18	23,47	26,83	31,48	34,65
IGFBP5	32,62	N/A	N/A	N/A	36,02	33,27	N/A	N/A
IL6	N/A	N/A	25,06	N/A	N/A	33,28	35,18	N/A
KLHL13	23,71	37,15	26,27	32,61	N/A	24,48	N/A	N/A
KLK3	34,9	N/A	37,94	23,28	23,63	21,43	N/A	N/A
LGALS4	N/A	N/A	31,41	N/A	39,07	32,43	N/A	N/A
LOXL1	25,79	25,27	25,19	32,21	N/A	26,84	39,73	N/A

MAPK1	23,19	25,19	24,33	24,24	24,58	22,62	N/A	N/A
MAX	24,96	31,3	24,52	40,56	30,71	29,47	37,28	N/A
MGMT	26,13	26,59	28,69	24,48	25,08	24,11	N/A	N/A
MKI67	23,02	23,71	23,4	N/A	N/A	23,81	N/A	N/A
MSX1	31,33	N/A	38,62	35,46	36,49	34,33	N/A	N/A
MTO1	23,11	25,04	23,8	23,79	23,97	20,29	36,88	36,24
NDRG3	23,27	24,6	23,69	27,82	28,55	21,92	N/A	N/A
NFKB1	24,32	24,61	26,15	30,49	31,49	23,2	26,82	27,78
NKX3-1	23,29	30,82	30,38	19,07	19,33	17,81	N/A	N/A
NRIP1	30,1	25,12	29,32	32,21	32,63	31,34	39,31	N/A
PDLIM4	27,24	31,12	24,69	37,8	34,13	36,3	N/A	N/A
PDPK1	24,29	24,15	22,35	25,79	26,52	22,71	40,66	N/A
PES1	24,39	28,68	28,6	27,14	27,95	24,38	N/A	N/A
PPP2R1B	24,88	28,1	22,61	31,12	30,92	22,75	N/A	N/A
PRKAB1	30,18	29,6	24,53	N/A	N/A	29,34	N/A	N/A
PTEN	N/A	N/A	N/A	24,52	24,88	23,06	N/A	N/A
PTGS1	32,5	40,97	38	35,77	N/A	33,56	N/A	35,6
PTGS2	39,35	N/A	32,39	N/A	34	33,31	38,72	N/A
RARB	25,03	39,89	36,38	24,29	25,06	27,04	N/A	N/A
RASSF1	31,96	39,11	34,63	N/A	36,32	33,67	N/A	N/A
RBM39	21,36	21,17	21	23,05	23,42	19,54	N/A	36,05
SCAF11	25,17	25,12	23,87	25,07	25,2	22,5	N/A	N/A
Sep7	22,03	24,18	23,35	26,99	27,41	23,07	32,93	37,65
SFRP1	33,74	40,61	34,16	N/A	40,5	35,58	40,61	N/A
SHBG	N/A	35,87	N/A	27,59	27,89	29,48	N/A	N/A
SLC5A8	N/A	N/A	N/A	36,7	38,15	32,8	N/A	N/A
SOCS3	32,29	33,58	35,82	N/A	N/A	36,2	N/A	N/A
SOX4	N/A	38,95	N/A	N/A	N/A	35,31	N/A	N/A
SREBF1	31,21	31,16	31,03	32,54	33,45	27,92	N/A	N/A
STK11	32	33,11	31,95	32,91	33,59	28,98	36,65	N/A
SUPT7L	23,02	22,89	22,31	22,09	22,37	20,93	37,73	36,53
TFPI2	19,92	23,82	20,76	N/A	N/A	37	N/A	N/A
TGFB111	27,83	32,15	33,04	N/A	34,71	36,29	N/A	N/A
TIMP2	21,29	21,84	21,29	25,12	25,53	25,44	N/A	N/A
TIMP3	33,25	36,21	33,72	37,37	37,4	37,05	38,1	40,35
TMPRSS2	N/A	32,77	31,05	20,57	21,05	21,14	N/A	N/A
TNFRSF10D	34,67	N/A	32,5	31,93	32,48	27,26	N/A	N/A
TP53	31,2	33,49	31,44	29,99	31,14	23,74	29,88	31,47
USP5	24,14	27,64	24,3	24,9	25,16	22,84	N/A	N/A
VEGFA	21,25	21,39	22,29	21,28	21,51	18,85	32,44	34,86
ZNF185	28,54	29,85	24,79	37,92	N/A	31,02	N/A	N/A
ACTB	18,04	19,98	18,91	20,21	20,44	18,05	22,48	23,73
B2M	21,1	23,77	21,29	22,37	22,82	20,84	19,99	21,28
GAPDH	17,05	19,49	18,62	19,29	19,64	16,28	22,98	25,7
HPRT1	22,06	23,49	22,39	31,71	31,75	21,12	31,03	30,9
RPLP0	15,18	16,5	15,81	15,94	16,18	12,46	19,51	21,37

HGDC	33,97	40,79	37,52	N/A	33,28	30,03	31,08	34,03
RTC	N/A	N/A	N/A	38,71	N/A	38,55	39,64	37,97
RTC	N/A	40,51	40,52	40,39	N/A	N/A	38,73	N/A
RTC	N/A	40,31	N/A	N/A	40,24	40,61	N/A	37,95
PPC	21,85	21,87	21,23	21,66	21,77	22,67	22,09	22,01
PPC	21,77	21,69	21,22	21,58	21,69	22,67	21,98	21,79
PPC	22,01	21,83	21,37	21,71	21,9	22,7	22,11	22

Supplement Table 2: Expression profile of breast cancer cell lines and leukocytes

	Leuko1	Leuko2	468	468	468	SKBR3	SKBR3	SKBR3
ADAM17	N/A	28,65	22,61	23,3	22,59	23,25	23,11	22,24
CTSD	29,61	28,83	21,32	22,28	20,35	19,49	19,64	18,3
HDAC2	N/A	27,87	20,34	20,44	19,72	21,05	20,8	19,56
MET_1	N/A	N/A	24,74	23,4	24,19	23,78	23,73	23,54
PARP	28,45	26,01	21,29	22,35	21,34	19,89	19,51	18,55
TOP2A	29,97	N/A	26,48	21,45	25,58	20,12	19,59	18,54
CCNE2	N/A	N/A	25,43	31,34	27,78	27,68	27,86	26,19
GAPDH	N/A	24,75	18,11	18,77	17,23	17,1	16,37	15,02
YWHAZ	26,24	24,61	19,82	20,07	19,14	20,77	20,62	18,76
AKT2	30,39	28,69	24,14	25,82	23,77	23,38	22,76	21,84
EGFR	N/A	N/A	19,33	20,06	18,95	N/A	N/A	N/A
IBSP_1	N/A	N/A	N/A	N/A	N/A	28,66	27,2	29,29
MRP2	N/A	N/A	27,96	N/A	28,7	27,93	31,25	26,9
PGR	N/A	N/A	N/A	N/A	N/A	N/A	N/A	N/A
TP53	27,62	26,59	21,34	21,9	21,06	21,54	21,7	20,24
PPIC	N/A	N/A	21,81	22,22	21,69	23,63	23,31	22,93
GUSB	N/A	30,54	24,48	25,28	24,12	23,21	23,27	21,74
ALDH	N/A	N/A	28,01	N/A	N/A	25,68	26,13	24,38
EPCAM	N/A	N/A	20,07	20,03	19,13	20,06	19,79	19,11
IGFR	N/A	27,79	25,98	26,15	25,59	24,78	25,57	23,51
MRP1	N/A	27,6	26,85	25,56	24,35	23,07	22,85	22,59
PI3KCA	N/A	28,58	25,11	25,54	24,54	23,5	22,61	21,7
Twist1	30,19	34,03	N/A	N/A	N/A	25,68	27,43	26,77
SLC6A8	N/A	N/A	26,94	27,89	27,34	23,94	23,48	22,29
HPRT1	N/A	28,07	23,43	24,08	23,13	23,15	23,62	N/A
AURKA	N/A	N/A	27,43	22,61	26,79	22,5	21,42	20,13
ERBB2	N/A	N/A	N/A	N/A	N/A	17,23	16,66	16,32
KI67	N/A	N/A	23,81	21,51	24,21	20,6	21,32	20,79
MRP4	28,91	31,94	26,81	27,69	25,62	27,02	26,09	25,28
PTEN	27,1	26,64	23,66	23,6	22,26	23,25	22,85	22,14
UPA	N/A	N/A	N/A	N/A	28,93	N/A	N/A	N/A
Hjurp	N/A	N/A	N/A	23,93	28,14	24,12	24,79	23,05
PPIA	24,52	24,2	17,77	18,1	16,88	16,98	17,17	15,47

CCND1	N/A	N/A	22,96	24,04	22,44	22,29	21,64	20,66
ESR1	N/A	28,91	N/A	N/A	27,25	N/A	N/A	N/A
KIT_1	N/A	N/A	N/A	N/A	N/A	N/A	N/A	N/A
MRP5	N/A	N/A	25,6	27,01	25,72	22,8	23,04	21,97
CD45/PTPRC	25,55	22,87	N/A	N/A	N/A	N/A	N/A	N/A
VEGFA	N/A	N/A	24,08	25,33	24,02	23,43	23,32	22,84
EMP2	N/A	N/A	22,15	22,17	21,1	21,18	20,94	20,31
RPLP	23,73	21,64	18,02	19,35	17,52	17,42	17,83	15,96
CD24L4	28,85	27,77	17,28	18,28	16,38	18,78	18,45	17,45
VEGFR1	N/A	N/A	N/A	N/A	N/A	N/A	N/A	N/A
KRAS	27,31	27,83	23,23	23,03	22,5	22,57	21,76	21,27
MTOR	N/A	N/A	25,12	26,32	24,88	24,71	23,47	23,01
RAD51	N/A	N/A	23,54	25,56	27,08	23,39	22,76	22,12
VIM	26,41	24,01	N/A	N/A	27,55	N/A	N/A	N/A
MAL2	N/A	N/A	21,46	22,22	21,26	18,17	18,11	16,69
TBP	N/A	30,82	25,3	25,02	24,51	25,14	24,97	23,23
CD44_all	26,09	24,7	18,6	19,17	18,15	26,09	N/A	28,99
FOXO	N/A	29,07	23,91	24,42	22,85	25,62	24,93	23,35
KRT19	N/A	N/A	18,32	18,92	17,49	17,76	17,06	15,95
MUC1	N/A	N/A	22,74	22,98	21,71	21,37	21,41	20,31
SATB1	N/A	26,94	N/A	N/A	N/A	28,22	26,79	24,8
WHSC1L1	N/A	28,71	27,45	27,39	25,93	24,51	25,45	25,36
ACTB	24,23	21,67	17,84	18,99	18,17	17,63	17,46	16,08
TUBB	N/A	29,12	24,62	24,26	23,73	24,98	24,63	23,28
CDH1_1	N/A	N/A	24,03	23,61	22,7	N/A	N/A	N/A
H2AFZ	N/A	25,48	19,13	18,88	18,81	18,01	17,76	16,89
MCM4	N/A	N/A	24,08	24,81	24,26	23,82	23,24	21,65
Myc*	28,07	28,21	23,7	25,84	25,48	22,07	22,72	21,24
SCGB2A/MAM	N/A	N/A	N/A	N/A	25,78	19,61	19,06	17,41
WHSC1S1	35,68	27,64	26,69	25,07	26,37	26,21	25,09	23,66
B2M	23,21	20,81	19,55	19,71	19,47	20,4	20,79	18,97
UBC	28,06	25,19	22,58	22,09	21,23	20,23	17,62	18,98

Supplement Table 3: Expression profile of CTCs and Leukocytes from a breast cancer patient (Fig. 1 green arrows (4))

	CTC1	CTC3	CTC5	CTC6	CTC7	CTC8	CTC9	CTC10	CTC12	Leuko	Leuko2.2	Leuko4	Leuko3
ADAM17	N/A	N/A	28,2	31,32	26,5	28,5	N/A	26,4	N/A	N/A	28,65	N/A	27,57
CTSD	25,9	29,1	28,6	25,25	26,3	27	29,5	26	29,51	29,61	28,83	N/A	N/A
HDAC2	27,38	27,7	26,9	26,5	N/A	29,8	N/A	25,8	27,72	N/A	27,87	N/A	N/A
MET_1	N/A	N/A	N/A	N/A	N/A	N/A	N/A	N/A	N/A	N/A	N/A	N/A	N/A
PARP	26,6	27,4	25,8	25,09	25,7	26,2	28,5	25,1	26,77	28,45	26,01	N/A	27,74
TOP2A	N/A	N/A	26,4	N/A	N/A	N/A	N/A	N/A	N/A	29,97	N/A	N/A	N/A
CCNE2	N/A	N/A	28,2	N/A	N/A	N/A	N/A	28,8	N/A	N/A	N/A	N/A	N/A

GAPDH	23,58	24,3	24,4	22,71	23,7	21,3	26,3	22,6	23,12	N/A	24,75	28,38	24,84
YWHAZ	23,92	26,3	25,8	23,96	26,4	23,9	N/A	25,1	25,45	26,24	24,61	27,27	25,91
AKT2	29,8	N/A	26,7	27,17	N/A	28	N/A	27,8	28,1	30,39	28,69	N/A	29,33
EGFR	N/A	N/A	N/A	N/A	N/A	N/A	N/A	N/A	N/A	N/A	N/A	N/A	N/A
IBSP_1	N/A	N/A	N/A	N/A	N/A	N/A	N/A	N/A	N/A	N/A	N/A	N/A	N/A
MRP2	N/A	N/A	N/A	N/A	N/A	N/A	N/A	N/A	N/A	N/A	N/A	N/A	N/A
PGR	N/A	N/A	N/A	N/A	N/A	N/A	N/A	N/A	N/A	N/A	N/A	N/A	N/A
TP53	27,34	27,3	25,7	26,33	27,1	N/A	N/A	27,7	24,86	27,62	26,59	28,63	26,63
PPIC	26,11	N/A	26,3	25,34	27,9	25,4	26,7	25,4	27,87	N/A	N/A	N/A	N/A
GUSB	28,74	29,8	26,7	29,34	31	29,7	N/A	28,8	29,2	N/A	30,54	N/A	N/A
ALDH	N/A	N/A	N/A	N/A	N/A	N/A	N/A	N/A	N/A	N/A	N/A	N/A	N/A
EPCAM	24,11	25,9	24,5	23,36	25,4	24,7	27,8	23,4	26,21	N/A	N/A	N/A	N/A
IGFR	N/A	28	N/A	N/A	26,9	N/A	N/A	N/A	28,26	N/A	27,79	N/A	29,4
MRP1	N/A	N/A	N/A	N/A	N/A	28,5	N/A	N/A	N/A	N/A	27,6	28,17	28,3
PI3KCA	29,89	N/A	N/A	28,83	N/A	N/A	N/A	27,8	28,62	N/A	28,58	N/A	N/A
Twist1	N/A	N/A	N/A	N/A	36,1	N/A	N/A	N/A	N/A	30,19	34,03	N/A	29,47
SLC6A8	N/A	N/A	N/A	32,44	N/A	N/A	N/A	N/A	27,79	N/A	N/A	N/A	N/A
HPRT1	N/A	29,3	28,1	N/A	28	27,2	N/A	N/A	26,38	N/A	28,07	N/A	28,14
AURKA	N/A	N/A	N/A	N/A	N/A	N/A	N/A	N/A	N/A	N/A	N/A	N/A	N/A
ERBB2	29,72	N/A	26,3	26,42	N/A	N/A	N/A	N/A	25,89	N/A	N/A	N/A	27,79
KI67	N/A	N/A	25,2	N/A	N/A	N/A	N/A	N/A	N/A	N/A	N/A	N/A	N/A
MRP4	N/A	N/A	N/A	N/A	N/A	N/A	N/A	N/A	N/A	28,91	31,94	N/A	N/A
PTEN	25,44	28,6	26,4	24,68	26,2	25,4	N/A	25,6	27,02	27,1	26,64	N/A	N/A
UPA	N/A	N/A	N/A	N/A	N/A	N/A	N/A	N/A	N/A	N/A	N/A	N/A	N/A
Hjurp	N/A	N/A	27,5	N/A	N/A	N/A	N/A	N/A	N/A	N/A	N/A	N/A	N/A
PPIA	23,24	24,4	23,4	23,43	24,6	22,8	26,1	22,8	23,99	24,52	24,2	27,36	24,83
CCND1	26,44	26,4	26,7	24,52	25,9	N/A	28,6	23,6	25,61	N/A	N/A	N/A	N/A
ESR1	28,29	28,3	N/A	27,19	26,4	27,1	27,9	27,2	29,14	N/A	28,91	N/A	N/A
KIT_1	N/A	N/A	N/A	N/A	N/A	N/A	N/A	N/A	N/A	N/A	N/A	N/A	N/A
MRP5	28,51	N/A	N/A	28,51	N/A	27,2	N/A	26,2	26,74	N/A	N/A	N/A	26,88
CD45/PTPRC	N/A	27,4	N/A	N/A	N/A	28,6	N/A	N/A	N/A	25,55	22,87	25,04	23,71
VEGFA	N/A	28,7	28,3	28,59	28,4	28,2	N/A	N/A	26,84	N/A	N/A	N/A	28,75
EMP2	25,83	26	25,4	26,09	26,3	26,6	N/A	28,5	25,91	N/A	N/A	N/A	N/A
RPLP	21,01	23,3	22,7	22,01	21,1	21,8	24,7	22,3	22,07	23,73	21,64	25,55	23,21
CD24L4	22,83	25,8	26,1	22,93	26,4	23,9	28,3	24,4	25,31	28,85	27,77	27,92	N/A
VEGFR1	N/A	N/A	N/A	N/A	N/A	N/A	N/A	N/A	N/A	N/A	N/A	N/A	N/A
KRAS	26,1	27,8	28,1	28,5	27,8	27,3	30,7	28,4	26,15	27,31	27,83	N/A	29,23
MTOR	29,4	N/A	N/A	27,42	N/A	N/A	N/A	26,6	27,76	N/A	N/A	N/A	N/A
RAD51	28,71	27	N/A	N/A	N/A	31,9	N/A	N/A	N/A	N/A	N/A	N/A	N/A
VIM	N/A	27,9	N/A	N/A	N/A	27,2	N/A	N/A	N/A	26,41	24,01	26,38	24,32
MAL2	23,49	29,6	25,8	24,69	25,1	25,8	28,6	24,7	24,94	N/A	N/A	N/A	N/A
TBP	N/A	N/A	N/A	N/A	N/A	N/A	29,1	27,6	28,19	N/A	30,82	N/A	N/A
CD44_all	N/A	32,5	28,5	N/A	N/A	25	N/A	N/A	28,39	26,09	24,7	25,04	24,63
FOXO	N/A	N/A	N/A	N/A	28,8	29,2	N/A	N/A	29,12	N/A	29,07	N/A	N/A
KRT19	22,59	23,3	25,3	21,41	23	22,6	27,1	23	24,15	N/A	N/A	N/A	N/A
MUC1	N/A	31,5	N/A	N/A	N/A	33,3	N/A	36,2	N/A	N/A	N/A	N/A	N/A

SATB1	N/A	N/A	N/A	N/A	N/A	N/A	N/A	N/A	N/A	N/A	26,94	N/A	29,34
WHSC1L1	27,61	N/A	N/A	N/A	N/A	N/A	N/A	28,2	N/A	N/A	28,71	N/A	N/A
ACTB	22,59	24,2	24	21,13	25,2	22,6	26,2	23,4	22,6	24,23	21,67	24,87	23,07
TUBB	28,16	29,4	30,9	27,23	N/A	26,8	N/A	29,1	N/A	N/A	29,12	28,88	N/A
CDH1_1	25,17	26,7	25,6	24,92	28,1	28,5	28,3	26,6	26,22	N/A	N/A	N/A	N/A
H2AFZ	26,54	25	23,2	23,71	28,2	23,3	26,4	24,1	24,9	N/A	25,48	26,41	26,22
MCM4	N/A	N/A	29,2	N/A	30,3	27,2	N/A	27,3	N/A	N/A	N/A	N/A	N/A
Myc*	30,05	29	36,8	30,04	N/A	29,3	N/A	N/A	N/A	28,07	28,21	29,6	28,5
SCGB2A/MAM	18,91	21,6	21	17,64	19,1	25,2	20	25,1	20,32	N/A	N/A	N/A	N/A
WHSC1S1	26,68	34	N/A	26,39	28,4	N/A	N/A	28,3	N/A	35,68	27,64	N/A	N/A
B2M	22,57	21,7	22	20,94	21,6	23,4	24,4	21,1	23,24	23,21	20,81	23,37	21,2
UBC	24,64	26	26	24,38	26	23,3	28,2	25,3	24,92	28,06	25,19	28,15	27,09

Supplementary Table 4: Expression profile of CTCs from a prostate cancer patient (Fig. 1 blue arrows (1))

	CTC1	CTC2	CTC3	CTC4	CTC5	CTC6	CTC7	CTC8
ACACA	23,92	29,61	25,01	30,41	N/A	26,32	31,43	29,75
AKT1	28,15	31,66	26,56	27,83	28	26,42	28,77	29,26
APC	N/A	N/A	25,81	N/A	39,2	N/A	N/A	N/A
AR	24,1	N/A	25,45	30,11	38,36	23,49	31,44	29,75
ARNTL	N/A	33,18	27,68	N/A	N/A	30,3	N/A	N/A
BCL2	24,09	32,64	26,01	33,06	32,72	23,4	32,44	34,97
CAMKK1	N/A	28,8	N/A	N/A	N/A	30,62	40,67	N/A
CAMSAP1	25,4	20,06	22,85	22,87	N/A	24,78	N/A	29,44
CASP3	33,01	27,54	23,94	33,15	N/A	24,77	N/A	24,19
CAV1	N/A	21,89	N/A	N/A	N/A	N/A	N/A	N/A
CAV2	N/A	40,9	40,7	38,48	N/A	39,08	37,78	N/A
CCNA1	N/A	N/A	33,51	32,55	N/A	N/A	N/A	N/A
CCND1	26,77	29,3	25,11	33,1	N/A	28,21	32,14	28,7
CCND2	29,52	27,87	22,8	N/A	40	22,66	N/A	31,53
CDH1	22,48	23,2	24,3	25,91	39,44	23,7	32,53	24,76
CDKN2A	23,68	20,34	20,4	32,54	28,82	22,53	33,23	30,9
CLN3	23,66	N/A	21,14	24,66	N/A	22,04	N/A	22,61
CREB1	32,94	24,65	23,12	31,88	N/A	N/A	N/A	N/A
DAXX	31,22	40,81	28,09	32,8	38,12	N/A	33,16	N/A
DDX11	27,32	40,69	29,09	38,47	39,54	29,67	N/A	38,72
DKK3	35,39	25,29	32,01	N/A	32,43	N/A	37,94	34,93
DLC1	N/A	N/A	40,06	N/A	32,28	N/A	39,56	N/A
ECT2	23,88	N/A	24,05	36,24	31,75	30,55	34,1	39,08
EDNRB	N/A	19,75	N/A	40,3	N/A	N/A	N/A	N/A
EGFR	25,81	27	40,93	40,11	30,28	33,43	31,28	N/A
EGR3	40,94	23,71	38,7	37,28	37,92	N/A	40,38	N/A
ERG	N/A	N/A	39,19	39,85	N/A	N/A	N/A	N/A
ETV1	30,78	32,57	N/A	31,99	N/A	32,48	N/A	N/A
FASN	26,46	20,69	25,31	30,42	38,66	26,86	28,41	25,61

FOXO1	26,08	21,55	25,68	27,71	36,05	N/A	N/A	26,8
GCA	24,61	N/A	22,12	25,3	N/A	23,92	N/A	30,65
GNRH1	N/A	29,12	N/A	N/A	N/A	30,04	N/A	N/A
GPX3	N/A	N/A	35,11	N/A	N/A	40,03	N/A	34,37
GSTP1	N/A	27,44	N/A	N/A	31,4	37,68	N/A	N/A
HAL	N/A	29,24	32,53	N/A	33,85	35,02	34,4	N/A
HMGCR	22,51	22,26	21,73	24,52	37,38	22,23	32,64	32,21
IGF1	N/A	40,78	N/A	N/A	N/A	40,72	N/A	N/A
IGFBP5	N/A	29,88	N/A	N/A	N/A	39,15	N/A	N/A
IL6	37,33	30,72	N/A	N/A	40,58	39,1	N/A	N/A
KLHL13	27,63	16,45	24,46	39,38	N/A	N/A	N/A	N/A
KLK3	20,86	35,78	18,95	23,74	32,65	20,43	26,89	24,26
LGALS4	32,76	N/A	30,07	N/A	N/A	N/A	N/A	33,45
LOXL1	29,52	N/A	40,2	37,65	38,48	33,6	39,05	40,11
MAPK1	24,12	N/A	23,49	24,82	32,06	27,66	29,33	32,82
MAX	33,23	N/A	29,29	N/A	31,66	30,16	31,12	33,12
MGMT	27,06	23,09	27,23	31,1	31,53	25,84	31,04	29,37
MKI67	N/A	36,31	N/A	31,91	36,8	33,1	38,66	N/A
MSX1	31,95	N/A	28,27	N/A	N/A	36,3	N/A	34,4
MTO1	22,2	N/A	21,64	N/A	36,28	23,31	N/A	21,13
NDRG3	27,28	32,11	N/A	40,59	N/A	25,09	31,69	23,64
NFKB1	23,9	31,62	23,65	26,14	36,64	23,48	N/A	27,22
NKX3-1	17,21	40,07	17,62	23,22	N/A	17,46	31,1	20,18
NRIP1	30,01	27,1	31,44	26	39,39	35,18	32,12	23,66
PDLIM4	34,24	N/A	40,03	37,5	38,57	37,04	N/A	33,33
PDPK1	22,71	20,45	22,69	24,42	N/A	23,32	32,5	29,42
PES1	30,1	N/A	24,41	30,6	N/A	27,4	N/A	24,91
PPP2R1B	25,04	25,55	22,46	27,66	N/A	23,85	32,22	31,45
PRKAB1	N/A	38,28	26,81	N/A	32,25	25,41	N/A	N/A
PTEN	21,9	N/A	21,09	N/A	N/A	21,42	N/A	23,57
PTGS1	N/A	N/A	N/A	N/A	N/A	N/A	39,86	40,03
PTGS2	33,85	28,02	N/A	N/A	N/A	N/A	N/A	N/A
RARB	24,22	N/A	23,6	N/A	N/A	23,3	N/A	N/A
RASSF1	31,72	N/A	31,44	30,24	39,76	36,35	N/A	N/A
RBM39	20,42	N/A	19,2	21,57	40,05	20,85	N/A	22,75
SCAF11	23,59	23,75	22,41	24,28	36,31	25,09	31,33	22,56
Sep7	21,86		21,58	25,7	31,66	23,64	32,17	25,53
SFRP1	35,18	N/A	37,95	40,01	40,75	N/A	34,99	N/A
SHBG	N/A	31,53	34,61	37,72	N/A	N/A	40,13	N/A
SLC5A8	40,22	33,06	N/A	N/A	39,34	N/A	N/A	N/A
SOCS3	N/A	N/A	N/A	N/A	N/A	39,04	N/A	N/A
SOX4	39,06	27,43	35,84	N/A	39,43	35,91	N/A	33
SREBF1	28,56	N/A	25,55	27,37	N/A	28,12	33,1	25,87
STK11	31,52	N/A	26,89	32,77	38,86	30,98	35,9	30,91
SUPT7L	22,27	N/A	20,79	23,62	N/A	21,53	30,07	26,92
TFPI2	32,68	N/A	N/A	N/A	N/A	N/A	N/A	32,5

TGFB111	37,12	29,03	35,82	N/A	N/A	37,29	N/A	40,22
TIMP2	22,5	N/A	24,41	27,69	N/A	22,79	32	26,85
TIMP3	32,59	N/A	36,45	35,08	36,97	38,07	40,04	38,06
TMPRSS2	19,76	24,09	17,54	22,7	30,17	17,67	29,99	19,51
TNFRSF10D	N/A	19,77	N/A	N/A	39,89	39,29	N/A	N/A
TP53	29,29	N/A	26,01	N/A	38,08	27,9	32,26	31,25
USP5	25,35	39,25	23,46	32,92	N/A	23,62	N/A	30,15
VEGFA	22,21	35,21	19,37	20,38	40,97	21,01	33,56	25,27
ZNF185	N/A	N/A	N/A	33,17	39,27	N/A	39,17	N/A
ACTB	18,29	22,7	18	21,53	31,35	18,07	25,72	20,73
B2M	20,64	N/A	18,1	21,36	25,41	19,93	25,3	21,34
GAPDH	19,21	22,21	16,79	20,05	25,98	18,41	25,7	20,46
HPRT1	24,04	19,7	23,09	30,45	30,04	26,51	30,24	23,41
RPLP0	15,45	N/A	13,35	17,11	22,57	14,62	21,75	16,3
HGDC	31,71	N/A	33,87	40,27	33,16	34,51	36,81	N/A
RTC	N/A	N/A	N/A	36,38	38,08	N/A	40,21	N/A
RTC	N/A	N/A	N/A	N/A	40,37	N/A	N/A	N/A
RTC	N/A	N/A	N/A	N/A	N/A	N/A	N/A	N/A
PPC	20,33	31,3	19,97	19,93	19,34	20,12	20,17	20,35
PPC	20,34	36,42	19,97	19,87	19,29	20,15	20,18	20,28
PPC	20,54	19,87	20,13	20,03	19,43	20,33	20,34	20,47

Supplementary Table 5: Expression profile of CTCs from a prostate cancer patient (Fig. 1 grey arrows (2))

	CTC1	CTC2	CTC3	CTC4	CTC6	CTC7	CTC8
AGR2	25,8	26,08	27,28	25,57	29,22	28,31	25,36
AHR	24,79	28,57	26,41	27,79	25,66	N/A	25,02
TUBB	30,39	28,81	34,43	N/A	N/A	N/A	28,4
ACTB	23,68	25,3	26,41	23,89	26,27	24,84	23,35
YWHAZ	24,58	25,07	27,57	26,03	29,16	26,07	25,79
B2M	24,19	23,39	24,48	23,44	26,45	25,01	22,87
UBC	25	23,85	25,27	24,84	26,31	26,37	25,05
TBP	N/A	N/A	N/A	N/A	N/A	N/A	N/A
AR	26,84	27,78	27,4	28,63	28,43	29,24	26,94
RPLP	21,7	21,96	23,43	22,36	22,52	22,37	22,62
CDH2	N/A	N/A	N/A	N/A	N/A	N/A	N/A
ANXA2R	31,05	N/A	N/A	N/A	29,44	N/A	N/A
GUSB	N/A	27,31	N/A	30,12	N/A	29,09	N/A
HPRT1	28,6	26,79	29,13	N/A	29,08	26,03	N/A
ADAM17	N/A	N/A	N/A	N/A	N/A	N/A	N/A
AKT2	28,27	N/A	N/A	N/A	N/A	27,78	N/A
ALDH	N/A	N/A	N/A	N/A	N/A	N/A	N/A

AURKA	N/A	N/A	N/A	N/A	N/A	N/A	N/A
CCND1	25,82	28,47	27,73	26,41	27,68	27,09	28,22
CD24L4	25,19	26,64	N/A	24,61	26,9	26,2	N/A
ARV7	29,45	N/A	N/A	29	N/A	N/A	28,81
AKR1C3	N/A	N/A	N/A	N/A	N/A	N/A	N/A
CYP11A1	N/A	N/A	N/A	N/A	N/A	N/A	N/A
CYP17A1	N/A	N/A	N/A	N/A	N/A	N/A	N/A
CD44_all	N/A	N/A	N/A	N/A	N/A	N/A	24,32
CDH1_1	25,44	26,62	28,82	26,82	28,07	27,59	N/A
CTSD	28,76	27,98	N/A	28,05	N/A	N/A	27,37
EGFR	30,76	27,92	N/A	N/A	N/A	N/A	N/A
EPCAM	26,09	25,21	26,35	25,24	26,81	26,33	25,36
ERBB2	25,99	27,03	27,43	29,68	N/A	29,26	27,96
ESR1	N/A	N/A	N/A	N/A	N/A	N/A	N/A
VEGFR1	N/A	N/A	N/A	N/A	N/A	N/A	N/A
CDH11	N/A	N/A	N/A	N/A	N/A	N/A	N/A
CYP19A1	N/A	N/A	N/A	N/A	N/A	N/A	N/A
BCL2	N/A	N/A	N/A	N/A	N/A	N/A	N/A
DDR1	31,03	N/A	N/A	N/A	N/A	N/A	N/A
FOXO	N/A	N/A	N/A	N/A	N/A	N/A	28,71
H2AFZ	24,76	23,98	25,79	25,1	24,41	23,63	23,84
HDAC2	26,64	25,56	N/A	26,33	N/A	25,62	N/A
IBSP_1	N/A	N/A	N/A	N/A	N/A	N/A	N/A
IGFR	N/A	N/A	N/A	N/A	N/A	N/A	N/A
KI67	N/A	26,26	N/A	N/A	26,95	25,36	N/A
KIT_1	N/A	N/A	N/A	N/A	N/A	N/A	N/A
TUBB3	N/A	N/A	N/A	N/A	N/A	N/A	N/A
CXCR4	N/A	N/A	N/A	N/A	N/A	N/A	26,36
ESR2	N/A	N/A	N/A	N/A	N/A	N/A	N/A
FOLH1	22,46	23,44	25,2	24,09	25,57	25,21	25,29
NCOA1	N/A	N/A	N/A	N/A	N/A	N/A	N/A
KRT19	26	26,83	26,27	26,22	N/A	28,31	26,43
MCM4	28,59	28,45	N/A	N/A	N/A	27,41	N/A
MET_1	N/A	N/A	N/A	N/A	N/A	N/A	N/A
MRP2	N/A	N/A	N/A	N/A	N/A	N/A	N/A
MRP1	N/A	28,01	N/A	N/A	N/A	N/A	N/A
MRP4	28,18	25,84	N/A	26,89	29,14	29,83	27,91
MRP5	29,22	N/A	N/A	N/A	N/A	N/A	N/A
MTOR	N/A	N/A	N/A	28,14	N/A	N/A	N/A
NES	N/A	N/A	N/A	N/A	N/A	N/A	N/A
KLK3	25,36	27,02	26,88	26,76	28,72	28,9	27,15
MCL1	27,38	26,35	28,56	25,97	27,08	27,64	25,37
MDK	36,83	N/A	N/A	N/A	36,19	33,17	N/A
MUC1	N/A	29,18	N/A	N/A	N/A	N/A	N/A
Myc_6	32,77	N/A	N/A	N/A	N/A	N/A	32,11
PARP	26,29	26,23	28,81	29,55	26,75	25,1	26,8

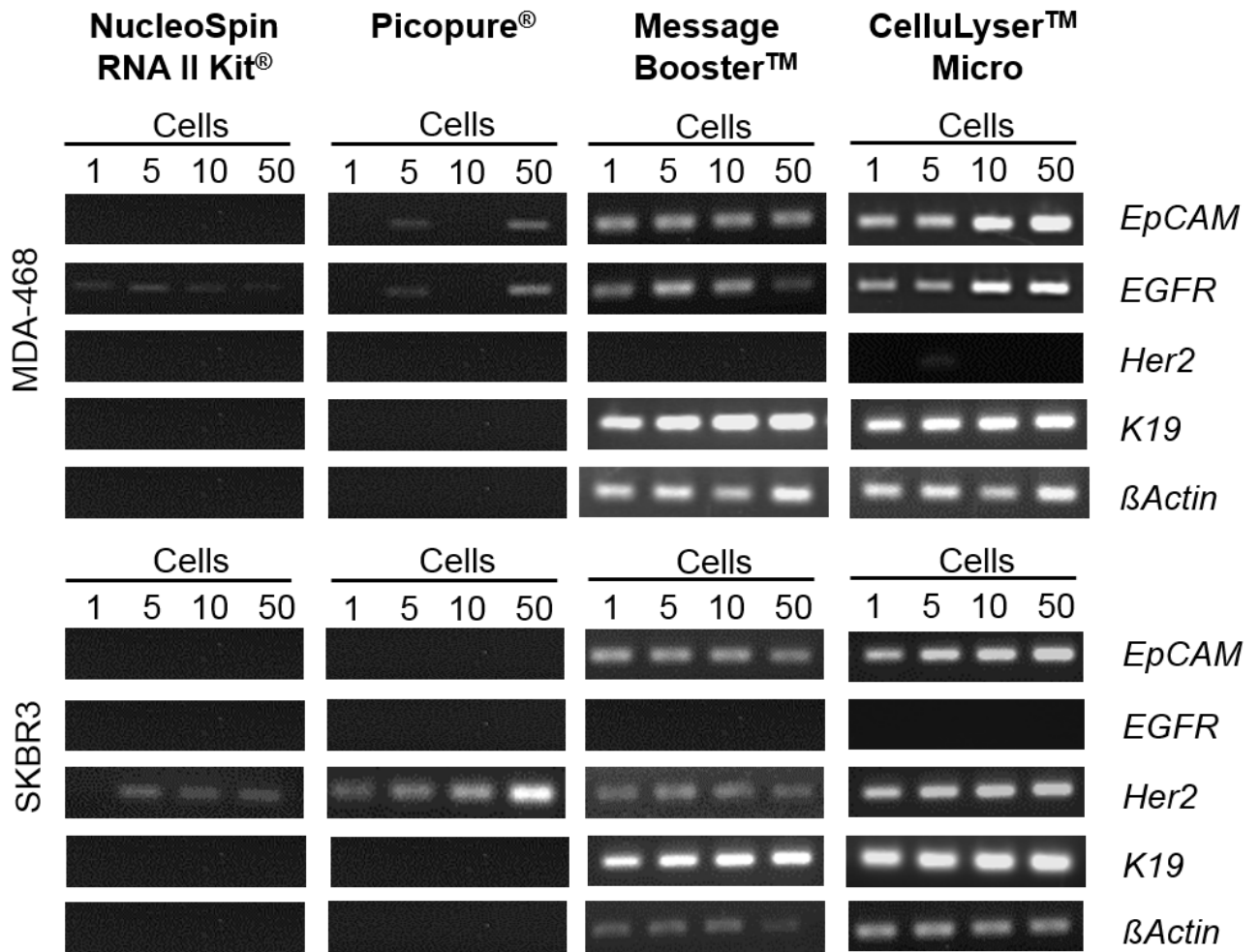
PGR	N/A	N/A	N/A	N/A	N/A	N/A	N/A
PI3KCA	N/A	N/A	28,87	N/A	N/A	N/A	N/A
PTEN	26,95	N/A	N/A	28,28	N/A	28,42	25,39
CD45 / PTPRC	N/A	N/A	N/A	N/A	N/A	N/A	N/A
RAD51	N/A	28,68	29,27	N/A	27,41	27,07	N/A
RUNX2	N/A	N/A	N/A	N/A	N/A	N/A	N/A
SRD5A1	29,12	N/A	N/A	N/A	N/A	N/A	28,12
STAT3	27,48	N/A	N/A	27,06	28,08	N/A	25,55
SNAI1	N/A	N/A	N/A	N/A	N/A	N/A	N/A
SATB1	N/A	N/A	N/A	N/A	N/A	N/A	N/A
SCGB2A / MAM	N/A	N/A	N/A	N/A	N/A	N/A	N/A
TOP2A	30,36	N/A	N/A	29,47	26,35	27,27	27,13
TP53	25,73	29,5	28,24	28,54	N/A	27,33	N/A
Twist1	28,16	N/A	N/A	N/A	N/A	N/A	N/A
UPA	N/A	N/A	N/A	N/A	N/A	N/A	N/A
TACSTD2	27,59	28,6	30,17	29,35	29,05	29,62	27,49
VIM	N/A	N/A	N/A	N/A	N/A	27,42	23,1
SHH	N/A	N/A	N/A	N/A	N/A	N/A	N/A
SPINK1	N/A	N/A	N/A	N/A	N/A	N/A	26,19
PROM1	N/A	N/A	N/A	N/A	N/A	N/A	N/A
TNFSF11	N/A	N/A	N/A	N/A	N/A	N/A	N/A
WHSC1L1_L1	N/A	N/A	N/A	N/A	N/A	N/A	N/A
WHSC1S1_S1	N/A	N/A	N/A	29,31	N/A	27,66	N/A
CCNE2	N/A	N/A	N/A	N/A	27,79	N/A	29
PPIC	29,07	27,68	N/A	N/A	N/A	N/A	N/A
SLC6A8	29,59	N/A	N/A	N/A	30,46	N/A	N/A
Hjurp	N/A	N/A	N/A	N/A	N/A	N/A	N/A
EMP2	28,9	34,85	N/A	N/A	N/A	27,41	N/A
MAL2	27,1	27,08	29,18	26,94	28,18	38,09	26,84
PTCH1	N/A	N/A	N/A	N/A	N/A	N/A	N/A
XIAP	29,34	N/A	N/A	27,98	29,3	N/A	N/A
POU5F1	31,65	N/A	N/A	31,04	27,92	N/A	28,4
PSCA	N/A	N/A	N/A	N/A	N/A	N/A	N/A

Supplementary Table 6: Expression profile of two CTCs from a breast cancer patient (Fig. 1 orange arrows (3))

	CTC Profil	CTC Parsortix
ACKR3	N/A	32,09
AICDA	N/A	38,17
BCL2	34,05	32,48
BCL2L1	32,24	31,1
CCL18	33,45	31,64
CCL2	35,79	35,69
CCL20	32,64	31,53
CCL21	36,23	32,5

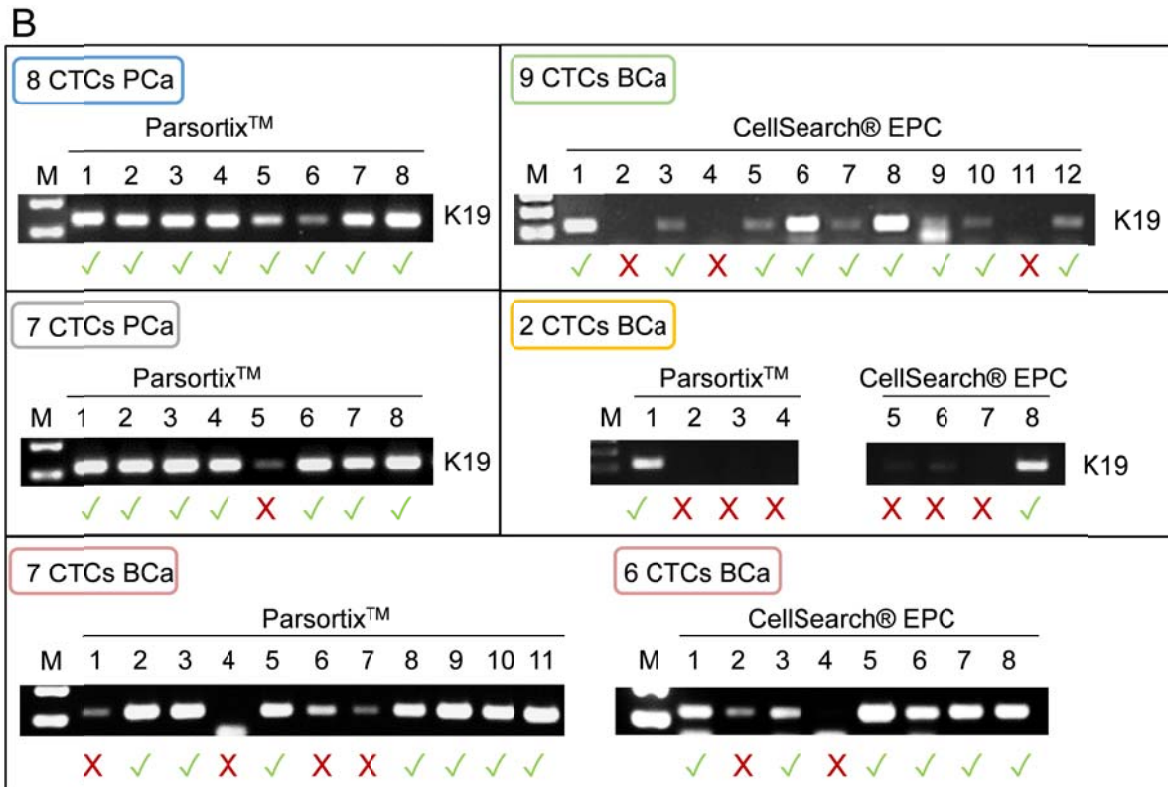
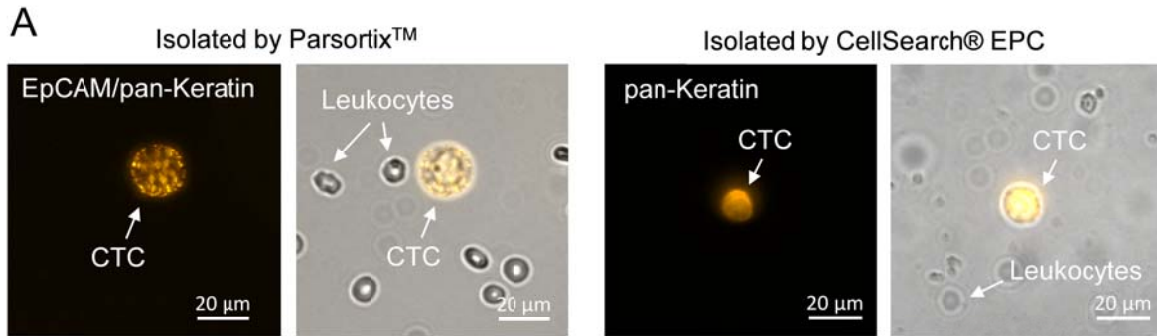
CCL22	N/A	N/A
CCL28	38,65	N/A
CCL4	23,52	18,79
CCL5	28,87	33,31
CCR1	40,81	N/A
CCR10	33,11	32,87
CCR2	38,46	35,58
CCR4	34,5	N/A
CCR7	N/A	N/A
CCR9	N/A	35,01
CD274	35,31	N/A
CSF1	37,14	32,77
CSF2	34,3	32,48
CSF3	33,05	34,56
CTLA4	N/A	34,23
CXCL1	32,49	29,45
CXCL10	36,04	N/A
CXCL11	36,22	N/A
CXCL12	31,15	30,16
CXCL2	36,13	26,73
CXCL5	N/A	35,88
CXCL9	27,12	32,9
CXCR1	34,64	36,45
CXCR2	32,35	31,67
CXCR3	N/A	37,71
CXCR4	38,18	N/A
CXCR5	N/A	37,88
EGF	33,4	36,37
EGFR	33	30,8
FASLG	33,08	31,07
FOXP3	N/A	30,91
GBP1	33,75	27,21
GZMA	N/A	32,22
GZMB	32,45	31,67
HIF1A	N/A	32,38
HLA-A	35,53	36,52
HLA-B	34,35	33,58
HLA-C	23,78	21,91
IDO1	35,27	34,33
IFNG	32,47	30,54
IGF1	32,15	30,43
IL10	31,98	29,33
IL12A	N/A	32,9
IL12B	N/A	37,5
IL13	N/A	32,21
IL15	33,49	24,29
IL17A	N/A	35,13
IL1A	N/A	37,21

IL1B	N/A	22,62
IL2	35,41	34,34
IL23A	N/A	36,24
IL4	34,58	31,92
IL6	34,6	33,29
IL8	N/A	24,89
IRF1	37,44	31,54
KITLG	34,58	N/A
MICA	N/A	N/A
MICB	37,95	30,65
MIF	26,61	22,83
MYC	30,86	24,23
MYD88	32,16	24,12
NFKB1	N/A	29,26
NOS2	33,18	31,27
PDCD1	34,9	33,12
PTGS2	N/A	33,1
SPP1	34,22	31,6
STAT1	26,61	27,28
STAT3	N/A	33,65
TGFB1	35,26	24,45
TLR2	36,04	34,88
TLR3	N/A	32,21
TLR4	N/A	35,1
TNF	N/A	28,1
TNFSF10	30,89	26,1
TP53	32,08	30,43
VEGFA	N/A	23,59
ACTB	25,01	26,75
B2M	23,12	22,76
GAPDH	24,53	24,33
HPRT1	31,32	30,94
RPLP0	22,57	21,03
HGDC	N/A	33,28
RTC	N/A	N/A
RTC	37,56	N/A
RTC	N/A	N/A
PPC	21,95	22,12
PPC	21,85	22,12
PPC	22,07	22,29



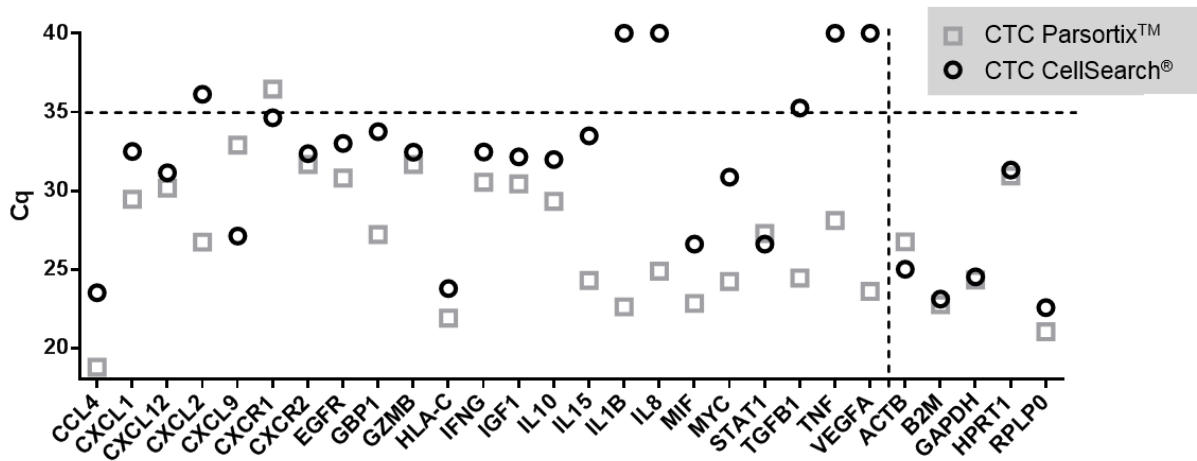
Supplement Fig. 1 Qualitative PCR.

1, 5, 10, or 50 MDA-468 or SKBR3 breast cancer cells were spiked directly into lysis buffer and processed either with the NucleoSpin RNA II Kit®, the Picopure RNA Isolation Kit® or the MessageBooster Kit™. Tumor cell specific transcripts (*EpCAM*, *EGFR*, *ERBB2*, and *k19*) together with *β-Actin* as house-keeping gene were amplified by qualitative PCR. Ethidium bromide stained-agarose gel electrophoresis was performed to visualize the PCR products.



Supplement Fig. 2 Qualitative PCR for single CTC RNA analysis of EpCAM / pan-keratin stained cells amplifying *k19* transcripts.

(A) Isolated EpCAM / pan-keratin-positive CTCs from cancer patients. (B) *k19* expression profile of the CTCs after micromanipulation. CTCs displaying an intense signal for *k19* were verified as a tumor cell and used for further multi-marker profiling as indicated by a green clamp (✓).



Supplement Fig. 3 Comparison of CTCs captured with either CellSearch® or Parsortix™ from the same patient.

Cells were analyzed using the MessageBooster Kit™ in combination with the RT² PreAmp and Profiler Cancer Inflammation & Immunity Crosstalk PCR Array. The average Cq value for each gene is shown separately. Missing values were replaced by 37.